

Dynamics of Polynomial Chaplygin Gas Warm Inflation

Abdul Jawad *

Department of Mathematics, COMSATS Institute of Information
Technology, Lahore-54000, Pakistan.

Shahid Chaudhary †

Department of Mathematics, Sharif College of Engineering
and Technology, Lahore-54000, Pakistan.

Nelson Videla ‡

Instituto de Física, Pontificia Universidad Católica de Valparaíso.
Avda. Universidad 330, Curauma, Valparaíso, Chile.

Abstract

In the present work, we study the consequences of considering a recently proposed polynomial inflationary potential in the context of the generalized, modified, and generalized cosmic Chaplygin gas models. In addition, we consider dissipative effects by coupling the inflation field to radiation, i.e., the inflationary dynamics is studied in the warm inflation scenario. We take into account a general parametrization of the dissipative coefficient Γ for describing the decay of the inflaton field into radiation. By studying the background and perturbative dynamics in the weak and strong dissipative regimes of warm inflation separately for the positive and negative quadratic and quartic potentials, we obtain expressions for the most relevant inflationary observables as the scalar power spectrum, the scalar spectral, and the tensor-to-scalar ratio. We construct the trajectories in the $n_s - r$ plane

*abduljawad@ciitlahore.edu.pk, jawadab181@yahoo.com

†shahidpeak00735@gmail.com

‡nelson.videla@pucv.cl

for several expressions of the dissipative coefficient and compare with the two-dimensional marginalized contours for (n_s, r) from the latest Planck data. We find that our results are in agreement with WMAP9 and Planck 2015 data.

Keywords: Warm inflation; Chaplygin gas models; Generalized dissipative regime; Quadratic and quartic potentials; Inflationary scenario.

1 Introduction

The anisotropies observed in the cosmic microwave background (CMB) are compatible with an adiabatic primordial scalar perturbation which is nearly Gaussian with a nearly scale-invariant power spectrum [1]. Cosmic inflation is the most successful theoretical framework in describing the very early stages of universe and also solves some shortcomings of the hot big-bang model, such as horizon, flatness and monopole [2] problems. However, the key feature of inflation is that it may be able to generate a causal mechanism to explain the large scale structure (LSS) of the universe [3] and the origin of the anisotropies observed in the CMB, since primordial density perturbations may be sourced from quantum fluctuations of the inflaton scalar field during the inflationary expansion. The standard cold inflation scenario [4]-[7] is divided into two regimes: the slow-roll and reheating phases. In the slow-roll period the universe undergoes an accelerated expansion as the potential energy of the inflaton field dominates over its kinetic energy and all interactions of the inflaton scalar field with other field degrees of freedom are typically neglected. Subsequently, a reheating period is invoked to end the brief acceleration. During reheating, kinetic energy of the inflaton field becomes comparable to its potential energy and by transferring its energy to massless particles, it oscillates around the minimum of the potential. After reheating, the universe is filled with relativistic particles and then the universe enters in the radiation big-bang epoch.

Alternatively, there is another dynamical mechanism for obtain a successful slow-roll inflation, i.e., the warm inflation scenario [8]-[12]. As opposed to standard cold inflation, warm inflation has the essential feature that a reheating phase is avoided at the end of the accelerated expansion due to the decay of the inflaton into radiation and particles during the slow-roll phase. However, the key difference is the origin of the density fluctuations. In the warm inflation scenario, a thermalized radiation component is present at

temperature T , which $T > H$, where H is the Hubble rate. In this way, the inflaton fluctuations $\delta\phi$ are predominantly thermal instead quantum [8]-[12].

Regarding standard cold inflation, Linde [13] introduced the concept of chaotic inflation in order to interpret the initial conditions for scalar field driving inflation which may help in solving the persisting problems of the old inflation models. In this model, the inflaton potential was chosen to be quadratic or quartic form, i.e. $\frac{m^2}{2}\phi^2$ or $\frac{\lambda}{4}\phi^4$, terms that are always present in the scalar potential of the Higgs sector in all renormalizable gauge field theories [14] in which the gauge symmetry is spontaneously broken via the Englert-Brout-Higgs mechanism [15, 16]. Such models are interesting for their simplicity, and has become one of the most favored, because they predict a significant amount of tensor perturbations due to the inflaton field gets across the trans-Planckian distance during inflation [17].

After introducing chaotic inflation, several works have been done in this direction. Herrera [18] discussed the warm inflation by assuming the chaotic potential in loop quantum cosmology and found consistency of results with observational data. The warm inflation was also investigated by del Campo and Herrera [19] driving by a scalar field with canonical kinetic term and a power-law dependence in the inflaton field for the dissipative coefficient, i.e., $\Gamma \propto \phi^n$, in the generalized Chaplygin gas (GCG) scenario. Further, Setare and Kamali investigated warm inflation driving by a tachyonic field and assumed the scale factor evolves according to intermediate [20] and loga-mediate [21] models. On the other hand, Bastero-Gill et al. [22] obtained analytic expressions for the dissipative coefficient in supersymmetric (SUSY) models and found that their results provide a realization of warm inflation in SUSY field theories. After, Bastero-Gill et al. [23] have also explored chaotic inflation by assuming the quartic potential. On the other hand, Herrera et al. studied intermediate inflation in the context of GCG using standard and tachyon scalar field models [24]. More recently, in Ref.[25], it was studied the dynamics of warm inflation in a modified Chaplygin gas (MCG).

Panotopoulos and Videla [26] discussed the warm inflation by assuming the quartic potential and an inflaton decay rate proportional to temperature and found that their results are in agreement with the latest Planck data, obtaining a lower value for the tensor-to-scalar ratio compared to the cold inflation scenario. Going further, several authors have investigated the warm inflation scenario in various alternative/modified theories of gravity [27, 28]. Moreover, a new family of inflation models is being developed named as shaft inflation [29]. In Ref.[30], the authors have developed inflationary parameters

by considering shaft potential and tachyon scalar field and found that their results are consistent with current observational data. Recently, Kobayashi and Seto [31] investigated the polynomial warm inflation and reported that their results are consistence with BICEP2 and Planck data.

The main goal of the present paper is to study the consequences of considering a polynomial inflationary potential in the context of the generalized, modified, and generalized cosmic Chaplygin gas models. In addition, we consider dissipative effects by coupling the inflation field to radiation, i.e., the inflationary dynamics will be studied in the warm inflation scenario. We take into account a general parametrization of the dissipative coefficient Γ for describing the decay of the inflaton field into radiation. The outline of the paper is as follows: In the next section, we provide the basic set of equations describing the warm inflationary scenario. In section **3**, **4** and **5**, we obtain the several inflationary observables in view of GCG, modified Chaplygin gas (MCG), and generalized cosmic Chaplygin gas (GCCG) models for positive/negative quadratic and quartic potentials. In section **6**, we summarize our findings and present our conclusions.

2 Basics of warm inflation scenario

2.1 Background evolution

The Friedmann equation for flat FRW universe in the presence of standard scalar field and a radiation fluid takes the following form

$$H^2 = \frac{1}{3M_p^2} (\rho_\phi + \rho_\gamma), \quad (1)$$

where $M_p = \frac{1}{\sqrt{8\pi G}}$ is the reduced Planck mass. The energy density of standard scalar field can be defined as $\rho_\phi = \dot{\phi}^2/2 + V(\phi)$ where dots represent derivative with respect to cosmic time. On the other hand, ρ_γ corresponds to the energy density of radiation fluid. The corresponding conservation equations for both standard scalar field and radiations turn out to be

$$\dot{\rho}_\phi + 3H(\rho_\phi + p_\phi) = -\Gamma\dot{\phi}^2, \quad \dot{\rho}_\gamma + 4H(\rho_\gamma) = \Gamma\dot{\phi}^2, \quad (2)$$

where p_ϕ denotes the pressure of standard scalar field, given by $p_\phi = \dot{\phi}^2/2 - V(\phi)$. By replacing the expressions for energy densities for the scalar field as

well as radiation in the first conservation equation, we get

$$\ddot{\phi} + (3H + \Gamma)\dot{\phi} + V' = 0, \quad (3)$$

where the primes denote derivatives with respect to ϕ . On the other hand, $\Gamma\dot{\phi}$ denotes the interaction term between the scalar field and radiation, whereas Γ is the responsible for the decay of the scalar field into radiation. This inflaton decay rate may depend on scalar field and temperature of thermal bath, or both quantities, or even it can be a constant. During warm inflation, the production of radiation is quasi-stable, i.e., $\dot{\rho}_\gamma \ll 4H\rho_\gamma$ and $\dot{\rho}_\gamma \ll \Gamma\dot{\phi}^2$ [3, 32]-[35]. This implies that energy density related to scalar field dominates over the energy density of radiation field and hence, the equations of motion under slow-roll approximation turn out to be

$$3H(1 + R)\dot{\phi} \simeq -V', \quad 4H\rho_\gamma \simeq \Gamma\dot{\phi}^2, \quad (4)$$

where $R = \frac{\Gamma}{3H}$ characterizes two dissipative regimes such as weak ($R \ll 1$) and strong ($R \gg 1$). A general parametrization of the inflaton decay rate is given by

$$\Gamma = c \frac{T^n}{\phi^{n-1}}, \quad (5)$$

where c is a constant parameter and n is an integer [36, 37]. Several expressions for the dissipative coefficient, corresponding to different values of n , have been studied in the literature [38, 39]. On the other hand, the energy density of the radiation field can be written as $\rho_\gamma = C_* T^4$, with $C_* = \pi^2 g_*/30$ and g_* represents the number of relativistic degrees of freedom. In minimal SUSY standard model, $g_* = 228.75$ and $C_* \simeq 70$. By using Eq.(4) and $\rho_\gamma \propto T^4$, we may find an expression for the temperature of thermal bath which is given by

$$T = \left(\frac{\Gamma V'^2}{6^2 C_* H^3 (1 + R)^2} \right)^{\frac{1}{4}}. \quad (6)$$

The set of slow-roll parameters for warm inflation is given by [32]

$$\epsilon = \frac{-\dot{H}}{H^2}, \quad \eta = \frac{-\ddot{H}}{H\dot{H}}, \quad \beta = \frac{-1}{H} \frac{d}{dt}(\ln \Gamma). \quad (7)$$

The number of e -folds is defined as

$$N = \int_{t_*}^{t_{end}} H dt. \quad (8)$$

where t_* and t_{end} denote the moment when the cosmological scales crosses the Hubble-radius and the end of inflation, respectively.

2.2 Cosmological perturbations

In the warm inflation scenario, a thermalized radiation component is present with $T > H$, then the inflaton fluctuations $\delta\phi$ are predominantly thermal instead quantum. In this way, following Ref.[12], the amplitude of the power spectrum of the curvature perturbation is given by

$$\mathcal{P}_{\mathcal{R}} \simeq \left(\frac{H}{2\pi}\right) \left(\frac{3H^2}{V'}\right) (1+R)^{5/4} \left(\frac{T}{H}\right)^{1/2}, \quad (9)$$

where the normalization has been chosen in order to recover the standard cold inflation result when $R \rightarrow 0$ and $T \simeq H$.

By the other hand, the scalar spectral index n_s , to leading order in the slow-roll approximation, becomes

$$n_s = 1 + \frac{dP_{\mathcal{R}}}{d\ln k} \simeq 1 - \frac{9\epsilon}{4} + \frac{3\eta}{2} - \frac{9\beta}{4}, \quad (10)$$

while for the tensor-to-scalar ratio, we have that [12]

$$r \simeq \left(\frac{H}{T}\right) \frac{16\epsilon}{(1+R)^{5/2}}. \quad (11)$$

When a specific form of the scalar potential and the dissipative coefficient are considered, it is possible to study the background evolution under the slow-roll regime and the primordial perturbations in order to test the viability of warm inflation. In the following we will study a polynomial potential, which has quadratic and quartic powers of the inflaton scalar field. A generalized expressions for the polynomial potential is proposed in [31], given by

$$V = t_1 + t_2\phi^2 + t_4\phi^4. \quad (12)$$

Since it is not easy to deal with several parameters, for convenience, we consider terms up to ϕ^4 which might be motivated by the renormalizability for this potential in quantum field theory. Thus, we consider two kind of polynomial potentials:

- Negative quadratic and quartic potential

$$V = s - \frac{1}{2}\sigma^2\phi^2 + \frac{\lambda_*}{4}\phi^4, \quad V' = -\sigma^2\phi + \lambda_*\phi^3 \quad (13)$$

- Positive quadratic and quartic potential

$$V = \frac{1}{2}\sigma^2\phi^2 + \frac{\lambda_*}{4}\phi^4, \quad V' = \sigma^2\phi + \lambda_*\phi^3 \quad (14)$$

where s , λ_* and σ are arbitrary constants. In the following sections, we illustrate the inflationary parameters for above mentioned scenario in the presence of three Chaplygin gas models (GCG, MCG and GCCG) by assuming weak and strong dissipative regimes with the inflaton decay rate given by the generalized expression (5).

3 Generalized Chaplygin Gas Model

It is believed that the universe undergoes an accelerated expansion of the universe and an exotic component having a negative pressure, usually known as dark energy (DE), is responsible for this expansion. Several models have been already proposed to be DE candidates, such as cosmological constant [40], quintessence [41]-[43], k-essence [44]-[46], tachyon [47]-[49], phantom [50]-[52], Chaplygin gas [53], holographic DE [56], among others in order to modify the matter sector of the gravitational action. Despite the plenty of models, the nature of the dark sector of the universe, i.e. DE and dark matter, is still unknown. There exists another way of understanding the observed universe in which dark matter and DE are described by a single unified component. Particularly, CG contains the unification of DE and dark matter and behaves as a pressureless matter at the early times and like a cosmological constant at late times [53]. It is noted that CG describes the universe in agreement with current observations of cosmic acceleration. The GCG is the extended form of CG and its equation of state (EoS) is [53]

$$p_{gcg} = -\frac{C_1}{\rho_{gcg}^\alpha} \quad (15)$$

where p_{gcg} and ρ_{gcg} represent the pressure and energy density of GCG model, respectively, with $0 < \alpha \leq 1$ and C_1 is the positive constant [53]. Also, ρ_{gcg} can be obtained through conservation equation as follows

$$\rho_{gcg} = \left(C_1 + \frac{C_2}{a^{3(1+\alpha)}} \right)^{\frac{1}{1+\alpha}}, \quad (16)$$

here C_2 is positive constant after integration. In this way, the term proportional to a^{-3} is identified as the energy density of matter ρ_m .

In order to obtain inflation in the Chaplygin-like gas scenarios studied in the present work, we follow Ref.[54]. The energy density of matter ρ_m is identified with the contribution of the energy density associated to the standard scalar field ρ_ϕ through an extrapolation of Eq.(16), yielding

$$\rho_{gcg} = (C_1 + \rho_m^{1+\alpha})^{\frac{1}{1+\alpha}} \longrightarrow (C_1 + \rho_\phi^{1+\alpha})^{\frac{1}{1+\alpha}}. \quad (17)$$

In this sense, we will not consider Eq.(17) as a consequence of Eq.(16), but a non-covariant modification of gravity instead, resulting in a modified Friedmann equation, as it was pointed up in Ref.[55].

In this scenario, we consider a spatially flat universe which contains a self-interacting inflation field ϕ and a radiation field, then the Friedmann equation (1) turns out to be

$$H^2 = \frac{1}{3M_p^2} \left[(C_1 + \rho_\phi^{1+\alpha})^{\frac{1}{1+\alpha}} + \rho_\gamma \right]. \quad (18)$$

We stress that Friedmann equation (18) comes from a non-covariant modification of gravity. However, as it was pointed up in Ref.[54], it may assumed that the effect giving rise to Eq. (18) preserves diffeomorphism invariance in (3+1) dimensions, whence total stress-energy conservation follows.

During inflation, the energy density of the scalar field dominates the energy density of the radiation field, i.e., $\rho_\phi \gg \rho_\gamma$ which leads to $\rho_\phi \sim V$. Here we take $\alpha = 1$ for the sake of simplicity. Then the Friedmann equation (18) becomes

$$H^2 = \frac{1}{3M_p^2} \sqrt{C_1 + \rho_\phi^2} \sim \frac{1}{3M_p^2} \sqrt{C_1 + V^2}. \quad (19)$$

Further, we will construct the inflationary parameters under two cases of dissipative coefficient that is weak dissipative regime ($R \leq 1$) and strong dissipative regime ($R \geq 1$) for the present case of GCG.

3.1 Weak Dissipative Regime

For this case, temperature turns out to be $T = (\frac{cV'^2}{6^2 C_* H^3 \phi^{n-1}})^{\frac{1}{4-n}}$ in the presence of generalized dissipative coefficient $\Gamma = c \frac{T^n}{\phi^{n-1}}$. With this temperature

and weak dissipative regime condition, the slow roll parameters (7) in terms of potential (V) can be written as

$$\begin{aligned}\epsilon &= \frac{M_p^2 V V'^2}{2(C_1 + V^2)^{\frac{3}{2}}}, \quad \eta = \frac{M_p^2}{(C_1 + V^2)^{\frac{1}{2}}} \left(V'' + \frac{V'^2}{V} - \frac{3VV'^2}{2(C_1 + V^2)} \right), \\ \beta &= M_p^2 \left(2(C_1 + V^2)(2nV'' - nV'(n-1)\phi^{-1} - V'(4-n)(n-1) \right. \\ &\quad \times \left. \phi^{-1}) - 3nV'^2V \right) \left(2(C_1 + V^2)^{\frac{3}{2}}(4-n) \right)^{-1}.\end{aligned}$$

With the help of Eq.(8), the number of e-folds become

$$N = \frac{1}{M_p^2} \int_{\phi_{end}}^{\phi_e} \frac{\sqrt{C_1 + V^2}}{V'} d\phi.$$

Equations (9)-(11) provide the power spectrum, scalar spectral index and tensor-to-scalar ratio in terms of potential (V) as follow

$$\begin{aligned}\mathcal{P}_{\mathcal{R}} &= \left(\frac{\pi}{4} \right)^{\frac{1}{2}} \frac{9(C_1 + V^2)^{\frac{3(5-2n)}{4(4-n)}} c^{\frac{3}{4-n}}}{3^{\frac{3(5-2n)}{2(4-n)}} M_p^{\frac{3(5-2n)}{4-n}} V'^{\frac{6-3n}{4-n}} \phi^{\frac{(n-1)(4-n)+(n-1)(n+2)}{2(4-n)}} 6^{\frac{n+2}{4-n}} C_*^{\frac{n+2}{2(4-n)}}}, \\ n_s - 1 &= \frac{3M_p^2}{2(C_1 + V^2)^{\frac{1}{2}}} \left(\frac{-9VV'^2}{4(C_1 + V^2)} - \frac{3}{2} \left(2(C_1 + V^2) \left(2nV'' \right. \right. \right. \\ &\quad \left. \left. - nV'(n-1)\phi^{-1} - V'(4-n)(n-1)\phi^{-1} \right) - 3nV'^2V \right) \\ &\quad \times \left(2(C_1 + V^2)(4-n) \right)^{-1} + V'' + \frac{V'^2}{V}, \\ r &= \frac{32G V'^{\frac{6-3n}{4-n}} \phi^{\frac{(n-1)(4-n)+(n-1)(n+2)}{2(4-n)}} 6^{\frac{n+2}{4-n}} C_*^{\frac{n+2}{2(4-n)}} 3^{\frac{7-4n}{2(4-n)}} M_p^{\frac{7-4n}{4-n}}}{9c^{\frac{3}{4-n}} \pi^{\frac{3}{2}} (C_1 + V^2)^{\frac{7-4n}{4(4-n)}}}. \quad (20)\end{aligned}$$

For positive quadratic and quartic potential: The above expressions of r and n_s in terms of scalar field lead to

$$\begin{aligned}r &= 32G \left(\sigma^2 \phi + \lambda_* \phi^3 \right)^{\frac{6-3n}{4-n}} \phi^{\frac{(n-1)(4-n)+(n-1)(n+2)}{2(4-n)}} 6^{\frac{n+2}{4-n}} C_*^{\frac{n+2}{2(4-n)}} 3^{\frac{7-4n}{2(4-n)}} \\ &\quad \times M_p^{\frac{7-4n}{4-n}} \left(9c^{\frac{3}{4-n}} \pi^{\frac{3}{2}} \left(C_1 + \left(\frac{\sigma^2 \phi^2}{2} + \frac{\lambda_* \phi^4}{4} \right)^2 \right)^{\frac{7-4n}{4(4-n)}} \right)^{-1},\end{aligned}$$

$$\begin{aligned}
n_s - 1 &= \frac{3M_p^2}{2(C_1 + (\frac{\sigma^2\phi^2}{2} + \frac{\lambda_*\phi^4}{4})^2)^{\frac{1}{2}}} \left(-9(\frac{\sigma^2\phi^2}{2} + \frac{\lambda_*\phi^4}{4})(\sigma^2\phi \right. \\
&+ \lambda_*\phi^3)^2 \left(4(C_1 + (\frac{\sigma^2\phi^2}{2} + \frac{\lambda_*\phi^4}{4})^2) \right)^{-1} - \frac{3}{2} \left(2(C_1 + (\frac{\sigma^2\phi^2}{2} \right. \\
&+ \frac{\lambda_*\phi^4}{4})^2)(2n(\sigma^2 + 3\lambda_*\phi^2) - n(\sigma^2\phi + \lambda_*\phi^3)(n-1)\phi^{-1} \\
&- (\sigma^2\phi + \lambda_*\phi^3)(4-n)(n-1)\phi^{-1}) - 3n(\sigma^2\phi + \lambda_*\phi^3)^2 \\
&\times (\frac{\sigma^2\phi^2}{2} + \frac{\lambda_*\phi^4}{4})(2(2(C_1 + (\frac{\sigma^2\phi^2}{2} + \frac{\lambda_*\phi^4}{4})^2))(4 \\
&- n))^{-1} \left. \right) + (\sigma^2 + 3\lambda_*\phi^2) + \frac{(\sigma^2\phi + \lambda_*\phi^3)^2}{(\frac{\sigma^2\phi^2}{2} + \frac{\lambda_*\phi^4}{4})} \Big).
\end{aligned}$$

For negative quadratic and quartic potential: The expressions of r and n_s for negative potential turn out to be

$$\begin{aligned}
r &= \frac{32G(-\sigma^2\phi + \lambda_*\phi^3)^{\frac{6-3n}{4-n}} \phi^{\frac{(n-1)(4-n)+(n-1)(n+2)}{2(4-n)}} 6^{\frac{n+2}{4-n}} C_*^{\frac{n+2}{2(4-n)}} 3^{\frac{7-4n}{2(4-n)}} M_p^{\frac{7-4n}{4-n}}}{9c^{\frac{3}{4-n}} \pi^{\frac{3}{2}} \left(C_1 + \left(s - \frac{\sigma^2\phi^2}{2} + \frac{\lambda_*\phi^4}{4} \right)^2 \right)^{\frac{7-4n}{4(4-n)}}}, \\
n_s &= 1 + \frac{3M_p^2}{2(C_1 + (s - \frac{\sigma^2\phi^2}{2} + \frac{\lambda_*\phi^4}{4})^2)^{\frac{1}{2}}} \left(-9(s - \frac{\sigma^2\phi^2}{2} + \frac{\lambda_*\phi^4}{4}) \right. \\
&\times (-\sigma^2\phi + \lambda_*\phi^3)^2 (4(C_1 + (s - \frac{\sigma^2\phi^2}{2} + \frac{\lambda_*\phi^4}{4})^2))^{-1} - \frac{3}{2} \\
&\times \left(2(C_1 + (s - \frac{\sigma^2\phi^2}{2} + \frac{\lambda_*\phi^4}{4})^2)(2n(-\sigma^2 + 3\lambda_*\phi^2) - n \right. \\
&\times (-\sigma^2\phi + \lambda_*\phi^3)(n-1)\phi^{-1} - (-\sigma^2\phi + \lambda_*\phi^3)(4-n) \\
&\times (n-1)\phi^{-1}) - 3n(-\sigma^2\phi + \lambda_*\phi^3)^2 (s - \frac{\sigma^2\phi^2}{2} + \frac{\lambda_*\phi^4}{4}) \\
&\times (2(2(C_1 + (s - \frac{\sigma^2\phi^2}{2} + \frac{\lambda_*\phi^4}{4})^2))(4-n))^{-1} \left. \right) + (-\sigma^2 \\
&+ 3\lambda_*\phi^2) + \frac{(-\sigma^2\phi + \lambda_*\phi^3)^2}{(s - \frac{\sigma^2\phi^2}{2} + \frac{\lambda_*\phi^4}{4})} \Big).
\end{aligned}$$

3.2 Strong Dissipative Regime

In this case, the temperature becomes $T = (\frac{V'^2 \phi^{n-1}}{4cc_* H})^{\frac{1}{n+4}}$. The slow-roll parameters lead to

$$\begin{aligned}\epsilon &= \frac{M_p^2 V V'^2}{2R(C_1 + V^2)^{\frac{3}{2}}}, \quad \eta = \frac{M_p^2}{R(C_1 + V^2)^{\frac{1}{2}}} \left(V'' + \frac{V'^2}{V} - \frac{3VV'^2}{2(C_1 + V^2)} \right), \\ \beta &= \frac{nM_p^2}{(n+4)R} \left(\frac{4V''(C_1 + V^2) - VV'^2}{2(C_1 + V^2)^{\frac{3}{2}}} \right).\end{aligned}$$

The power spectrum, scalar spectral index and tensor-to-scalar ratio turn out to be

$$\begin{aligned}\mathcal{P}_{\mathcal{R}} &= \left(\frac{\pi}{4} \right)^{\frac{1}{2}} \frac{c^{\frac{23-5n}{10}} (C_1 + V^2)^{\frac{23-5n}{40}}}{V'^{\frac{8-5n}{5}} (4c_*)^{\frac{5n+2}{10}} M_p^{\frac{23-5n}{10}} 3^{\frac{23-5n}{20}}}, \\ n_s - 1 &= \left(\frac{3(4c_*)^{\frac{1}{5}}}{c^{\frac{4}{5}} V'^{\frac{2}{5}}} \right) \frac{(3M_p^2)^{\frac{2}{5}}}{2(C_1 + V^2)^{\frac{1}{5}}} \left(V'' + \frac{V'^2}{V} - \frac{9VV'^2}{4(C_1 + V^2)} \right) \\ &\quad - \frac{3(n)}{2(n+4)} \left(\frac{4V''(C_1 + V^2) - VV'^2}{2(C_1 + V^2)} \right) \\ r &= \frac{32GV'^{\frac{8-5n}{5}} \phi^{\frac{5(n-1)}{2}} (4c_*)^{\frac{5n+2}{10}} (C_1 + V^2)^{\frac{5n-3}{40}}}{\pi^{\frac{3}{2}} c^{\frac{23-5n}{10}} 3^{\frac{5n-3}{20}} M_p^{\frac{5n-3}{10}}}.\end{aligned}\tag{21}$$

For positive quadratic and quartic potential: The scalar spectral index and tensor-to-scalar ratio in case of strong dissipative regime turns out to be

$$\begin{aligned}r &= \frac{32G(\sigma^2 \phi + \lambda_* \phi^3)^{\frac{8-5n}{5}} \phi^{\frac{5(n-1)}{2}} (4c_*)^{\frac{5n+2}{10}} \left(C_1 + \left(\frac{\sigma^2 \phi^2}{2} + \frac{\lambda_* \phi^4}{4} \right)^2 \right)^{\frac{5n-3}{40}}}{\pi^{\frac{3}{2}} b^{\frac{23-5n}{10}} 3^{\frac{5n-3}{20}} M_p^{\frac{5n-3}{10}}} \\ n_s - 1 &= \left(\frac{3(4c_*)^{\frac{1}{5}}}{c^{\frac{4}{5}} (\sigma^2 \phi + \lambda_* \phi^3)^{\frac{2}{5}}} \right) \frac{(3M_p^2)^{\frac{2}{5}}}{2(C_1 + (\frac{\sigma^2 \phi^2}{2} + \frac{\lambda_* \phi^4}{4})^2)^{\frac{1}{5}}} \left((\sigma^2 \right. \\ &\quad + 3\lambda_* \phi^2) + \frac{(\sigma^2 \phi + \lambda_* \phi^3)^2}{(\frac{\sigma^2 \phi^2}{2} + \frac{\lambda_* \phi^4}{4})} - \frac{9(\frac{\sigma^2 \phi^2}{2} + \frac{\lambda_* \phi^4}{4})(\sigma^2 \phi + \lambda_* \phi^3)^2}{4(C_1 + (\frac{\sigma^2 \phi^2}{2} + \frac{\lambda_* \phi^4}{4})^2)} \\ &\quad \left. - \frac{3(n)}{2(n+4)} \left(4(\sigma^2 + 3\lambda_* \phi^2)(C_1 + (\frac{\sigma^2 \phi^2}{2} + \frac{\lambda_* \phi^4}{4})^2) \right) \right)\end{aligned}$$

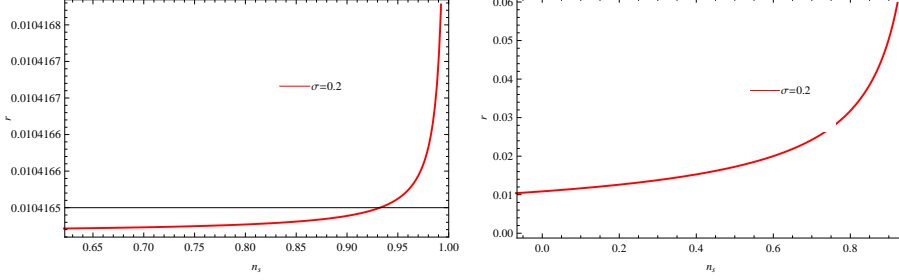


Figure 1: Plot of r versus n_s for GCG model in weak (left panel) and strong (right panel) dissipative regimes for positive potential with $n = 1$.

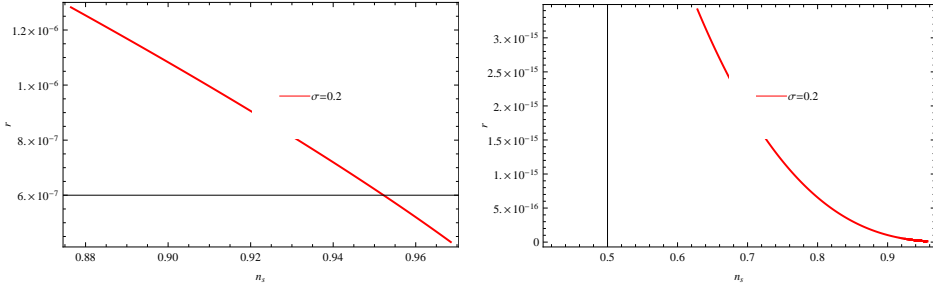


Figure 2: Plot of r versus n_s for GCG model in weak (left panel) and strong (right panel) dissipative regimes for positive potential with $n = -1$.

$$\begin{aligned}
& - \left(\frac{\sigma^2 \phi^2}{2} + \frac{\lambda_* \phi^4}{4} \right) (\sigma^2 \phi + \lambda_* \phi^3)^2 \left(2 \left(C_1 + \left(\frac{\sigma^2 \phi^2}{2} + \frac{\lambda_* \phi^4}{4} \right)^2 \right)^{-1} \right) \right). \quad (22)
\end{aligned}$$

By utilizing the value of negative quadratic and quartic potential and its derivative in the expressions (21) of the scalar spectral index and tensor-to-scalar ratio, we obtain

$$\begin{aligned}
r &= \frac{32G (-\sigma^2 \phi + \lambda_* \phi^3)^{\frac{8-5n}{5}} \phi^{\frac{5(n-1)}{2}} (4c_*)^{\frac{5n+2}{10}} (C_1 + (s - \frac{\sigma^2 \phi^2}{2} + \frac{\lambda_* \phi^4}{4})^2)^{\frac{5n-3}{40}}}{\pi^{\frac{3}{2}} c^{\frac{23-5n}{10}} 3^{\frac{5n-3}{20}} M_p^{\frac{5n-3}{10}}} \\
n_s &= 1 + \left(\frac{3(4c_*)^{\frac{1}{5}}}{c^{\frac{4}{5}} (-\sigma^2 \phi + \lambda_* \phi^3)^{\frac{2}{5}}} \right) \frac{(3M_p^2)^{\frac{2}{5}}}{2(C_1 + (s - \frac{\sigma^2 \phi^2}{2} + \frac{\lambda_* \phi^4}{4})^2)^{\frac{1}{5}}}
\end{aligned}$$

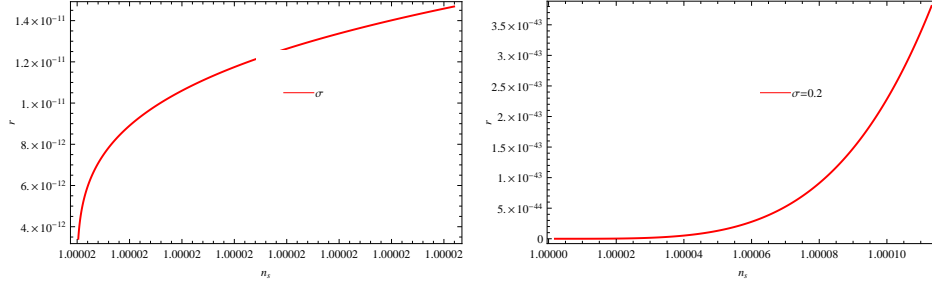


Figure 3: Plot of r versus n_s for GCG model in weak (left panel) and strong (right panel) dissipative regimes for positive potential with $n = -2$.

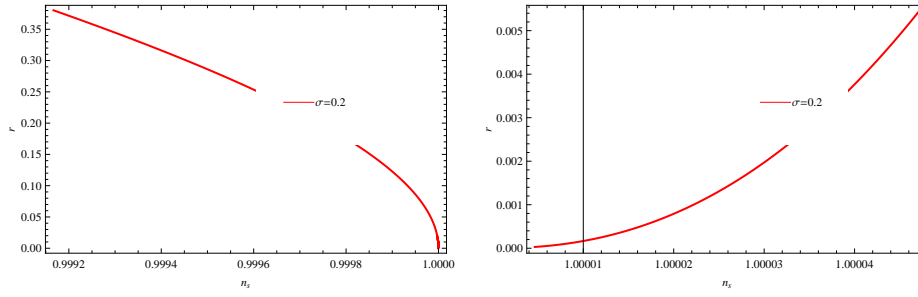


Figure 4: Plot of r versus n_s for GCG model in weak (left panel) and strong (right panel) dissipative regimes for negative potential with $n = 1$.

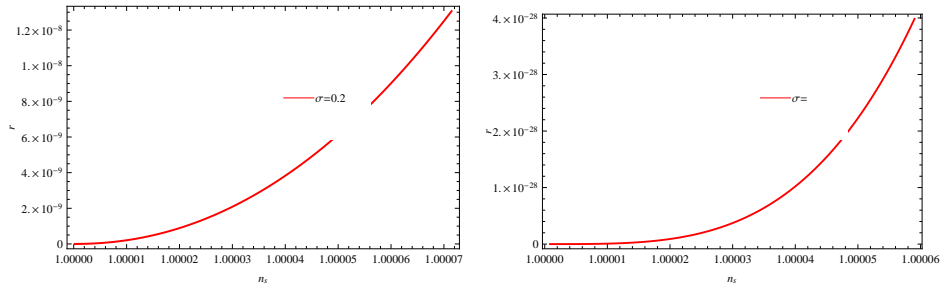


Figure 5: Plot of r versus n_s for GCG model in weak (left panel) and strong (right panel) dissipative regimes for negative potential with $n = -1$.

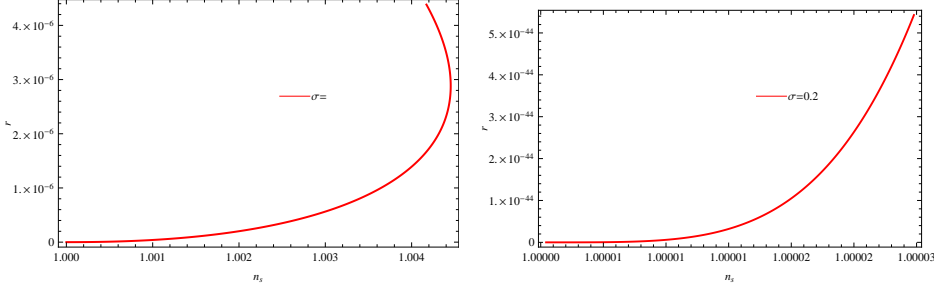


Figure 6: Plot of r versus n_s for GCG model in weak (left panel) and strong (right panel) dissipative regimes for negative potential with $n = -2$.

$$\begin{aligned}
& \times \left((-\sigma^2 + 3\lambda_*\phi^2) + \frac{(-\sigma^2\phi + \lambda_*\phi^3)^2}{(s - \frac{\sigma^2\phi^2}{2} + \frac{\lambda_*\phi^4}{4})} - 9(s - \frac{\sigma^2\phi^2}{2} \right. \\
& + \frac{\lambda_*\phi^4}{4})(-\sigma^2\phi + \lambda_*\phi^3)^2(4(C_1 + (s - \frac{\sigma^2\phi^2}{2} + \frac{\lambda_*\phi^4}{4})^2))^{-1} \\
& - \frac{3(n)}{2(n+4)} \left(4(-\sigma^2 + 3\lambda_*\phi^2)(C_1 + (s - \frac{\sigma^2\phi^2}{2} + \frac{\lambda_*\phi^4}{4})^2) \right. \\
& - (s - \frac{\sigma^2\phi^2}{2} + \frac{\lambda_*\phi^4}{4})(-\sigma^2\phi + \lambda_*\phi^3)^2(2(C_1 + (s - \frac{\sigma^2\phi^2}{2} \\
& + \frac{\lambda_*\phi^4}{4})^2))^{-1} \left. \left. \right) \right). \tag{23}
\end{aligned}$$

We plot the graphs of r and n_s for both weak and strong dissipative regimes by assuming the positive quadratic and quartic potential for three different values of $n = 1, -1, -2$, respectively as shown in Figures **1-3**. The other constant parameters appear in the model are assumed to be as follows: $M_p = 1, \alpha = 10^{-13}, C_1 = 10^{-45}, \lambda_* = 10^{-3}, c = 0.3, C_* = 70$. The constraints of inflationary parameters such as tensor-to-scalar ratio and spectral index are displayed in the Table **1(a)**. It is found that the results are compatible with WMAP9 [57] and Planck 2015 [58] which are given in Table **1**.

Table 1: WMAP9 [57] and Planck 2015 [58] data for r and n_s .

r (WMAP9)	n_s (WMAP9)	r (Planck 2015)	n_s (Planck2015)
< 0.13	0.972 ± 0.013	< 0.11	0.968 ± 0.006

Table 1(a): GCG Weak and Strong Dissipative Regimes with Positive Quadratic and Quartic Potential.

<i>Sr.No</i>	<i>n</i>	$r(W)$	$n_s(W)$	$r(S)$	$n_s(S)$
1	1	≤ 0.0104168	$0.98^{+0.01}_{-0.01}$	≤ 0.06	$0.90^{+0.06}_{-0.06}$
2	-1	$\leq 1.2 \times 10^{-6}$	$0.96^{+0.02}_{-0.02}$	$\leq 3.0 \times 10^{-15}$	$0.94^{+0.02}_{-0.02}$
3	-2	$\leq 1.4 \times 10^{-14}$	$1.00001^{+0.00001}_{-0.00001}$	$\leq 3.7 \times 10^{-43}$	$1.00011^{+0.00001}_{-0.00001}$

Figures 4-6 show the behavior of r and n_s for negative quadratic and quartic potential in weak and strong dissipative regimes. The parameters appear in the model attained the values $M_p = 1, s = 2, \alpha = 10^{-5}, C_1 = 10^{-45}, c = 0.3, C_* = 70, \lambda_* = 10^{-13}, c = 10^{-7}, G = 0.0398$. The result for negative quadratic and quartic potential are shown in the Table 1(b). The values of tensor-to-scalar ratio and spectral index are consistence with observational data WMAP9 [57] and Planck 2015 [58].

Table 1(b): GCG Weak and Strong Dissipative Regime with Negative Quadratic and Quartic Potential.

<i>Sr.No</i>	<i>n</i>	$r(W)$	$n_s(W)$	$r(S)$	$n_s(S)$
1	1	≤ 0.38	$1.0000^{+0.0001}_{-0.0001}$	≤ 0.0055	$1.0004^{+0.0001}_{-0.0001}$
2	-1	≤ 0.000041	$1.0031^{+0.0001}_{-0.0001}$	$\leq 4.0 \times 10^{-28}$	$1.000057^{+0.000001}_{-0.000001}$
3	-2	$\leq 4.5 \times 10^{-6}$	$1.0040^{+0.0001}_{-0.0001}$	$\leq 5.2 \times 10^{-44}$	$1.00002^{+0.00001}_{-0.00001}$

4 Modified Chaplygin Gas

The EoS of MCG is given as [59]

$$p_{mcg} = \zeta \rho_{mcg} - \frac{\xi}{\rho_{mcg}^\alpha}, \quad (24)$$

where p_{mcg} and ρ_{mcg} represent the pressure and energy density of MCG, respectively and $0 \leq \alpha \leq 1$, while ζ and ξ are positive constants. The

energy density ρ_{mcg} can be calculated by using energy conservation equation as follows

$$\rho_{mcg} = \left(C_3 + \frac{C_4}{a^{3(1+\alpha)(1+\zeta)}} \right)^{\frac{1}{1+\alpha}}, \quad (25)$$

here C_4 is an integration constant and $C_3 = \frac{\xi}{1+\zeta}$. In view of MCG, Friedmann equation takes the following form

$$H^2 = \frac{1}{3M_p^2} \left[(C_3 + \rho_\phi^{(1+\alpha)(1+\zeta)})^{\frac{1}{1+\alpha}} + \rho_\gamma \right]. \quad (26)$$

Under certain conditions as mentioned in GCG case, the above Friedmann equation reduces to

$$H^2 = \frac{1}{3M_p^2} (C_3 + \rho_\phi^{(1+\alpha)(1+\zeta)})^{\frac{1}{1+\alpha}} \sim \frac{1}{3M_p^2} (C_3 + V^{(1+\alpha)(1+\zeta)})^{\frac{1}{1+\alpha}}. \quad (27)$$

Next, we extract the inflationary parameters for both cases of dissipative coefficient.

4.1 Weak Dissipative Regime

Here, the temperature remains the same as in case of GCG while slow roll parameters turn out to be

$$\begin{aligned} \epsilon &= \frac{M_P^2(1+\zeta)V^{(1+\alpha)(1+\zeta)-1}V'^2}{2(C_3 + V^{(1+\alpha)(1+\zeta)})^{\frac{2+\alpha}{1+\alpha}}}, \quad \eta = \frac{M_p^2}{(C_3 + V^{(1+\alpha)(1+\zeta)})^{\frac{1}{1+\alpha}}} \left(2V'' \right. \\ &\quad \left. + \frac{V'^2((1+\alpha)(1+\zeta)-1)}{V} - \frac{V^{(1+\alpha)(1+\zeta)-1}V'^2(1+\alpha)(1+\zeta)}{(C_3 + V^{(1+\alpha)(1+\zeta)})} \right), \\ \beta &= M_p^2 \left((C_3 + V^{(1+\alpha)(1+\zeta)})2(2nV'' - nV'(n-1)\phi^{-1} - V' \right. \\ &\quad \times (4-n)(n-1)\phi^{-1})((2(4-n)(C_3 + V^{(1+\alpha)(1+\zeta)})^{\frac{2+\alpha}{1+\alpha}})^{-1} \\ &\quad \left. - \frac{3n(1+\zeta)V'^2V^{(1+\alpha)(1+\zeta)-1}}{2(4-n)(C_3 + V^{(1+\alpha)(1+\zeta)})^{\frac{2+\alpha}{1+\alpha}}} \right). \end{aligned}$$

Similarly, by using Eq.(8), the number of e-folds leads to

$$N = \frac{1}{M_P^2} \int_{\phi_{end}}^{\phi_*} \frac{(C_3 + V^{(1+\alpha)(1+\zeta)})^{\frac{1}{1+\alpha}}}{V'} d\phi. \quad (28)$$

With the help of Eq.(9)-(11), power spectrum, scalar spectral index and tensor-to-scalar ratio in the form of potential given by

$$\begin{aligned}
\mathcal{P}_{\mathcal{R}} &= \left(\frac{81\pi}{4} \right)^{\frac{1}{2}} \left(\frac{M_p^{\frac{6n-15}{4-n}} (C_3 + V^{(1+\alpha)(1+\zeta)})^{\frac{15-6n}{2(4-n)(1+\alpha)}} c^{\frac{3}{4-n}}}{3^{\frac{15-6n}{2(4-n)}} C_*^{\frac{n+2}{2(n+4)}} V'^{\frac{6-3n}{4-n}} 6^{\frac{n+2}{4-n}} \phi^{\frac{(n-1)(4-n)+(n-1)(n+2)}{2(4-n)}}} \right), \\
n_s - 1 &= \frac{3M_p^2}{2(C_3 + V^{(1+\alpha)(1+\zeta)})^{\frac{1}{1+\alpha}}} \left(\frac{V'^2((1+\alpha)(1+\zeta) - 1)}{V} \right. \\
&\quad - \frac{V^{(1+\alpha)(1+\zeta)-1} V'^2}{(C_3 + V^{(1+\alpha)(1+\zeta)})} \left(\frac{3}{4}(1+\zeta) + (1+\alpha)(1+\zeta) \right) \\
&\quad + 2V'' - \frac{3}{2} \left((C_3 + V^{(1+\alpha)(1+\zeta)}) 2(2nV'' - nV'(n \right. \\
&\quad - 1)\phi^{-1} - V'(4-n)(n-1)\phi^{-1} - 3n(1+\zeta) \\
&\quad \times V^{(1+\alpha)(1+\zeta)-1} V'^2) (2(4-n)(C_3 + V^{(1+\alpha)(1+\zeta)}))^{-1} \Bigg), \quad (29)
\end{aligned}$$

$$r = \frac{32GV'^{\frac{6-3n}{4-n}} \phi^{\frac{(n-1)(4-n)+(n-1)(n+2)}{2(4-n)}} 6^{\frac{n+2}{4-n}} C_*^{\frac{n+2}{2(4-n)}} 3^{\frac{7-4n}{2(4-n)}} M_p^{\frac{7-4n}{4-n}}}{9c^{\frac{3}{4-n}} \pi^{\frac{3}{2}} (C_3 + V^{(1+\alpha)(1+\zeta)})^{\frac{7-4n}{(4-n)(2+2\alpha)}}}. \quad (30)$$

For positive quadratic and quartic potential, we get the following expressions of r and n_s

$$\begin{aligned}
r &= \frac{32G \left(\sigma^2 \phi + \lambda_* \phi^3 \right)^{\frac{6-3n}{4-n}} \phi^{\frac{(n-1)(4-n)+(n-1)(n+2)}{2(4-n)}} 6^{\frac{n+2}{4-n}} C_*^{\frac{n+2}{2(4-n)}} 3^{\frac{7-4n}{2(4-n)}}}{9c^{\frac{3}{4-n}} \pi^{\frac{3}{2}} M_p^{\frac{4n-7}{4-n}} \left(C_3 + \left(\frac{1}{2} \sigma^2 \phi^2 + \frac{\lambda_*}{4} \phi^4 \right)^{(1+\alpha)(1+\zeta)} \right)^{\frac{7-4n}{(4-n)(2+2\alpha)}}}, \\
n_s - 1 &= \frac{3M_p^2}{2\{C_3 + (\frac{1}{2} \sigma^2 \phi^2 + \frac{\lambda_*}{4} \phi^4)^{(1+\alpha)(1+\zeta)}\}^{\frac{1}{1+\alpha}}} \left[(\sigma^2 \phi + \lambda_* \phi^3)^2 \{ (1+\alpha) \right. \\
&\quad \times (1+\zeta) - 1 \} \left(\frac{1}{2} \sigma^2 \phi^2 + \frac{\lambda_*}{4} \phi^4 \right)^{-1} - \left(\frac{1}{2} \sigma^2 \phi^2 \frac{\lambda_*}{4} \phi^4 \right)^{(1+\alpha)(1+\zeta)-1} \\
&\quad \times (\sigma^2 \phi + \lambda_* \phi^3)^2 \left\{ C_3 + \left(\frac{1}{2} \sigma^2 \phi^2 + \frac{\lambda_*}{4} \phi^4 \right)^{(1+\alpha)(1+\zeta)} \right\}^{-1} \\
&\quad \times \left(\frac{3}{4}(1+\zeta) + (1+\alpha)(1+\zeta) \right) + 2(\sigma^2 + 3\lambda_* \phi^2) - \frac{3}{2}
\end{aligned}$$

$$\begin{aligned}
& \times \left\{ 2 \left(C_3 + \left(\frac{1}{2} \sigma^2 \phi^2 + \frac{\lambda_*}{4} \phi^4 \right)^{(1+\alpha)(1+\zeta)} \right) \left(2n(\sigma^2 + 3\lambda_* \phi^2) \right. \right. \\
& - n(\sigma^2 \phi + \lambda_* \phi^3)(n-1)\phi^{-1} - (\sigma^2 \phi + \lambda_* \phi^3)(4-n)(n-1)\phi^{-1} \\
& - 3n(1+\zeta) \left(\frac{1}{2} \sigma^2 \phi^2 + \frac{\lambda_*}{4} \phi^4 \right)^{(1+\alpha)(1+\zeta)-1} (\sigma^2 \phi + \lambda_* \phi^3)^2 \\
& \times \left. \left. (2(4-n)(C_3 + \left(\frac{1}{2} \sigma^2 \phi^2 + \frac{\lambda_*}{4} \phi^4 \right)^{(1+\alpha)(1+\zeta)}))^{-1} \right) \right\} \Bigg]. \quad (31)
\end{aligned}$$

For negative quadratic and quartic potential, the relations of r and n_s lead to

$$\begin{aligned}
r &= \frac{32G(-\sigma^2 \phi + \lambda_* \phi^3)^{\frac{6-3n}{4-n}} \phi^{\frac{(n-1)(4-n)+(n-1)(n+2)}{2(4-n)}} 6^{\frac{n+2}{4-n}} C_*^{\frac{n+2}{2(4-n)}} 3^{\frac{7-4n}{2(4-n)}}}{9c^{\frac{3}{4-n}} \pi^{\frac{3}{2}} M_p^{\frac{4n-7}{4-n}} (C_3 + (s - \frac{1}{2} \sigma^2 \phi^2 + \frac{\lambda_*}{4} \phi^4)^{(1+\alpha)(1+\zeta)})^{\frac{7-4n}{(4-n)(2+2\alpha)}}}, \\
n_s - 1 &= \frac{3M_p^2}{2 \left\{ C_3 + \left(s - \frac{1}{2} \sigma^2 \phi^2 + \frac{\lambda_*}{4} \phi^4 \right)^{(1+\alpha)(1+\zeta)} \right\}^{\frac{1}{1+\alpha}}} \left[\left(-\sigma^2 \phi \right. \right. \\
& + \lambda_* \phi^3 \Big)^2 \{ (1+\alpha)(1+\zeta) - 1 \} \left(s - \frac{1}{2} \sigma^2 \phi^2 + \frac{\lambda_*}{4} \phi^4 \right)^{-1} \\
& - \frac{(s - \frac{1}{2} \sigma^2 \phi^2 + \frac{\lambda_*}{4} \phi^4)^{(1+\alpha)(1+\zeta)-1} (-\sigma^2 \phi + \lambda_* \phi^3)^2}{C_3 + (s - \frac{1}{2} \sigma^2 \phi^2 + \frac{\lambda_*}{4} \phi^4)^{(1+\alpha)(1+\zeta)}} \\
& \times \left(\frac{3}{4} (1+\zeta) + (1+\alpha)(1+\zeta) \right) + 2(-\sigma^2 + 3\lambda_* \phi^2) \\
& - \frac{3}{2} \left\{ \left(C_3 + (s - \frac{1}{2} \sigma^2 \phi^2 + \frac{\lambda_*}{4} \phi^4)^{(1+\alpha)(1+\zeta)} \right) 2 \left(2n(-\sigma^2 \right. \right. \\
& + 3\lambda_* \phi^2) - n(-\sigma^2 \phi + \lambda_* \phi^3)(n-1)\phi^{-1} - (-\sigma^2 \phi + \lambda_* \phi^3) \\
& \times (4-n)(n-1)\phi^{-1} \Big) - 3n(1+\zeta) \left(s - \frac{1}{2} \sigma^2 \phi^2 + \frac{\lambda_*}{4} \phi^4 \right)^{(1+\alpha)(1+\zeta)-1} \\
& \times (2(4-n)(C_3 + (s - \frac{1}{2} \sigma^2 \phi^2 + \frac{\lambda_*}{4} \phi^4)^{(1+\alpha)(1+\zeta)}))^{-1} \\
& \times \left. \left. (-\sigma^2 \phi + \lambda_* \phi^3)^2 \right\} \right]. \quad (32)
\end{aligned}$$

4.2 Strong Dissipative Regime

In this case, the slow roll parameters become

$$\begin{aligned}\epsilon &= \frac{M_P^2(1+\zeta)V^{(1+\alpha)(1+\zeta)-1}V'^2}{2R(C_3 + V^{(1+\alpha)(1+\zeta)})^{\frac{2+\alpha}{1+\alpha}}}, \quad \eta = \frac{M_p^2}{R(C_3 + V^{(1+\alpha)(1+\zeta)})^{\frac{1}{1+\alpha}}}(2V'' \\ &+ \frac{V'^2((1+\alpha)(1+\zeta)-1)}{V} - \frac{V^{(1+\alpha)(1+\zeta)-1}V'^2(1+\alpha)(1+\zeta)}{(C_3 + V^{(1+\alpha)(1+\zeta)})}, \\ \beta &= \frac{n}{R}M_p^2 \left(\frac{4V''(C_3 + V^{(1+\alpha)(1+\zeta)}) - (1+\zeta)V'^2V^{(1+\alpha)(1+\zeta)-1}}{2(n+4)(C_3 + V^{(1+\alpha)(1+\zeta)})^{\frac{2+\alpha}{1+\alpha}}} \right).\end{aligned}$$

The number of e-folds turn out to be

$$N = \frac{1}{M_P^2} \int_{\phi_{\text{end}}}^{\phi_*} \frac{(C_3 + V^{(1+\alpha)(1+\zeta)})^{\frac{1}{1+\alpha}}}{V'} R d\phi$$

The relations for perturbation, tensor-to-scalar ratio, spectral index can be obtained by utilizing Eq.(9)-(11) as follows

$$\begin{aligned}\mathcal{P}_{\mathcal{R}} &= \left(\frac{\pi}{4}\right)^{\frac{1}{2}} \frac{c^{\frac{9}{n+4}} (C_3 + V^{(1+\alpha)(1+\zeta)})^{\frac{9}{2(1+\alpha)(n+4)}}}{(4C_*)^{\frac{5n+2}{2(n+4)}} \phi^{\frac{5(n-1)(n+4)-(n-1)(5n+2)}{2(n+4)}} V'^{\frac{6-3n}{n+4}} M_p^{\frac{9}{n+4}} 3^{\frac{9}{2(n+4)}}}, \\ n_s - 1 &= \frac{3(4c_*)^{\frac{n}{n+4}} \phi^{\frac{(n+4)(n-1)-n(n-1)}{n+4}} 3^{\frac{2}{n+4}} M_p^{\frac{4}{n+4}}}{2c^{\frac{4}{n+4}} V'^{\frac{2n}{n+4}} (C_3 + V^{(1+\alpha)(1+\zeta)})^{\frac{2}{(1+\alpha)(n+4)}}} \left[\frac{V'^2}{V^1} \left((1+\alpha)(1+\zeta) \right. \right. \\ &\times \left. \left. -1 \right) - \frac{V^{(1+\alpha)(1+\zeta)-1}V'^2}{(C_3 + V^{(1+\alpha)(1+\zeta)})} \times \left(\frac{3}{4}(1+\zeta) + (1+\alpha)(1+\zeta) \right) \right. \\ &+ \left. 2V'' - \left(\frac{3n}{2} \left(4V''(C_3 + V^{(1+\alpha)(1+\zeta)}) - (1+\zeta)V'^2V^{(1+\alpha)(1+\zeta)-1} \right) \right. \right. \\ &\times \left. \left. \left(2(n+4)(C_3 + V^{(1+\alpha)(1+\zeta)}) \right)^{-1} \right) \right], \\ r &= \frac{32G(4C_*)^{\frac{5n+2}{10}} \phi^{\frac{5(n-1)}{2}} V'^{\frac{8-5n}{5}} (C_3 + V^{(1+\alpha)(1+\zeta)})^{\frac{5n-3}{20(1+\alpha)}}}{c^{\frac{23-5n}{10}} \pi^{\frac{3}{2}} 3^{\frac{5n-3}{20}} M_p^{\frac{5n-3}{10}}}.\end{aligned}$$

For positive quadratic and quartic potential, the tensor-to-scalar ratio and

scalar spectral index in terms of ϕ are given by

$$\begin{aligned}
r &= \frac{32G(4C_*)^{\frac{5n+2}{10}} \phi^{\frac{5(n-1)}{2}} \left(C_3 + \left(\frac{\sigma^2 \phi^2}{2} + \frac{\lambda_* \phi^4}{4} \right)^{(1+\alpha)(1+\zeta)} \right)^{\frac{5n-3}{20(1+\alpha)}}}{c^{\frac{23-5n}{10}} \pi^{\frac{3}{2}} 3^{\frac{5n-3}{20}} M_p^{\frac{5n-3}{10}} (\sigma^2 \phi + \lambda_* \phi^3)^{\frac{5n-8}{5}}}, \\
n_s - 1 &= \frac{3c^{\frac{-4}{n+4}} (4c_*)^{\frac{n}{n+4}} \phi^{\frac{(n+4)(n-1)-n(n-1)}{n+4}} 3^{\frac{2}{n+4}} M_p^{\frac{4}{n+4}}}{2(\sigma^2 \phi + \lambda_* \phi^3)^{\frac{2n}{n+4}} (C_3 + (\frac{1}{2}\sigma^2 \phi^2 + \frac{\lambda_* \phi^4}{4})^{(1+\alpha)(1+\zeta)})^{\frac{2}{(1+\alpha)(n+4)}}} \\
&\times \left[\frac{(\sigma^2 \phi + \lambda_* \phi^3)^2 ((1+\alpha)(1+\zeta) - 1)}{\frac{1}{2}\sigma^2 \phi^2 + \frac{\lambda_* \phi^4}{4}} - (\sigma^2 \phi + \lambda_* \phi^3)^2 \right. \\
&\times \left(\frac{1}{2}\sigma^2 \phi^2 + \frac{\lambda_* \phi^4}{4} \right)^{(1+\alpha)(1+\zeta)-1} \left(\left(\frac{1}{2}\sigma^2 \phi^2 + \frac{\lambda_* \phi^4}{4} \right)^{(1+\alpha)(1+\zeta)} \right. \\
&+ \left. C_3 \right)^{-1} \left(\frac{3}{4}(1+\zeta) + (1+\alpha)(1+\zeta) \right) + 2(\sigma^2 + 3\lambda_* \phi^2) \\
&- \frac{3n}{2} \left(4(\sigma^2 + 3\lambda_* \phi^2)(C_3 + (\frac{1}{2}\sigma^2 \phi^2 + \frac{\lambda_* \phi^4}{4})^{(1+\alpha)(1+\zeta)}) \right. \\
&- (1+\zeta)(\sigma^2 \phi + \lambda_* \phi^3)^2 (\frac{1}{2}\sigma^2 \phi^2 + \frac{\lambda_* \phi^4}{4})^{(1+\alpha)(1+\zeta)-1} \\
&\times \left. \left. (2(n+4)(C_3 + (\frac{1}{2}\sigma^2 \phi^2 + \frac{\lambda_* \phi^4}{4})^{(1+\alpha)(1+\zeta)}))^{-1} \right) \right]. \quad (33)
\end{aligned}$$

For negative quadratic and quartic potential, the tensor-to-scalar ratio and scalar spectral index in terms of ϕ lead to

$$\begin{aligned}
r &= 32G(4C_*)^{\frac{5n+2}{10}} \phi^{\frac{5(n-1)}{2}} (-\sigma^2 \phi + \lambda_* \phi^3)^{\frac{8-5n}{5}} (C_3 + (\frac{\sigma^2 \phi^2}{2} \\
&+ \frac{\lambda_* \phi^4}{4})^{(1+\alpha)(1+\zeta)})^{\frac{5n-3}{20(1+\alpha)}} (c^{\frac{23-5n}{10}} \pi^{\frac{3}{2}} 3^{\frac{5n-3}{20}} M_p^{\frac{5n-3}{10}})^{-1}. \\
n_s - 1 &= 3(4c_*)^{\frac{n}{n+4}} \phi^{\frac{(n+4)(n-1)-n(n-1)}{n+4}} 3^{\frac{2}{n+4}} M_p^{\frac{4}{n+4}} (2c^{\frac{4}{n+4}} (-\sigma^2 \phi \\
&+ \lambda_* \phi^3)^{\frac{2n}{n+4}} (C_3 + (s - \frac{1}{2}\sigma^2 \phi^2 + \frac{\lambda_* \phi^4}{4})^{(1+\alpha)(1+\zeta)})^{\frac{2}{(1+\alpha)(n+4)}})^{-1} \\
&\times \left(\frac{(-\sigma^2 \phi + \lambda_* \phi^3)^2 ((1+\alpha)(1+\zeta) - 1)}{s - \frac{1}{2}\sigma^2 \phi^2 + \frac{\lambda_* \phi^4}{4}} - (s - \frac{1}{2}\sigma^2 \phi^2 \right. \\
&+ \left. \frac{\lambda_* \phi^4}{4})^{(1+\alpha)(1+\zeta)-1} (-\sigma^2 \phi + \lambda_* \phi^3)^2 ((C_3 + (s - \frac{1}{2}\sigma^2 \phi^2 \right.
\end{aligned}$$

$$\begin{aligned}
& + \frac{\lambda_* \phi^4}{4})^{(1+\alpha)(1+\zeta)})^{-1} \left(\frac{3}{4}(1+\zeta) + (1+\alpha)(1+\zeta) \right) + 2 \\
& \times (-\sigma^2 + 3\lambda_* \phi^2) - \frac{3n}{2} \left(4(-\sigma^2 + 3\lambda_* \phi^2)(C_3 + (s \right. \\
& - \frac{1}{2}\sigma^2 \phi^2 + \frac{\lambda_* \phi^4}{4})^{(1+\alpha)(1+\zeta)}) - (1+\zeta)(-\sigma^2 \phi + \lambda_* \phi^3)^2 \\
& \times (s - \frac{1}{2}\sigma^2 \phi^2 + \frac{\lambda_* \phi^4}{4})^{(1+\alpha)(1+\zeta)-1}) \\
& \times \left. (2(n+4)(C_3 + (s - \frac{1}{2}\sigma^2 \phi^2 + \frac{\lambda_* \phi^4}{4})^{(1+\alpha)(1+\zeta)})^{-1}) \right) \Bigg). \quad (34)
\end{aligned}$$

For MCG model, the plots of r and n_s for both weak/strong dissipative regimes for both positive/negative quadratic and quartic potential for three different values of $n = 1, -1, -2$, respectively are shown in Figures **7-12**. The observed constraints of scalar ratio and spectral index are displayed in the Tables **2(a)** and **2(b)**. It is found that the results are compatible with WMAP9 [57] and Planck 2015 [58].

Table 2(a): MCG Weak and Strong Dissipative Regimes with Positive Quadratic and Quartic Potential.

<i>Sr.No</i>	n	$r(W)$	$n_s(W)$	$r(S)$	$n_s(S)$
1	1	≤ 0.005	$1.00001^{+0.00001}_{-0.00001}$	≤ 0.00025	$1.0000^{+0.0001}_{-0.00001}$
2	-1	≤ 0.05	$1.17^{+0.001}_{-0.001}$	≤ 0.00028	$1.034^{+0.001}_{-0.001}$
3	-2	≤ 0.000025	$0.98^{+0.01}_{-0.01}$	$\leq 2.5 \times 10^{-14}$	$0.9^{+0.1}_{-0.1}$

Table 2(b): MCG Weak and Strong Dissipative Regime with Negative Quadratic and Quartic Potential.

<i>Sr.No</i>	n	$r(W)$	$n_s(W)$	$r(S)$	$n_s(S)$
1	1	≤ 0.5	$1.0009^{+0.001}_{-0.001}$	≤ 0.0052	$1.00000^{+0.00001}_{-0.00001}$
2	-1	≤ 0.00007	$1.019^{+0.001}_{-0.001}$	≤ 0.00028	$1.034^{+0.001}_{-0.001}$
3	-2	$\leq 7.2 \times 10^{-6}$	$1.019^{+0.001}_{-0.001}$	$\leq 2.5 \times 10^{-8}$	$0.9^{+0.1}_{-0.1}$

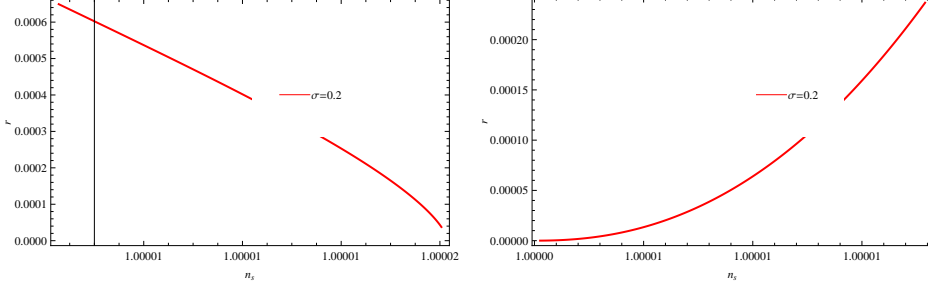


Figure 7: Plot of r versus n_s for MCG model in weak (left panel) and strong (right panel) dissipative regimes for positive potential with $n = 1$.

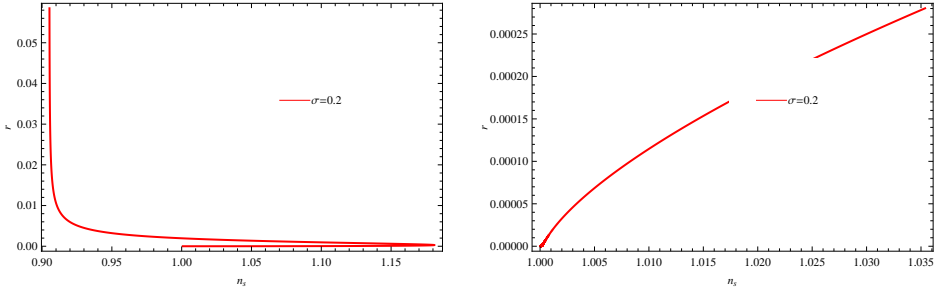


Figure 8: Plot of r versus n_s for MCG model in weak (left panel) and strong (right panel) dissipative regimes for positive potential with $n = -1$.

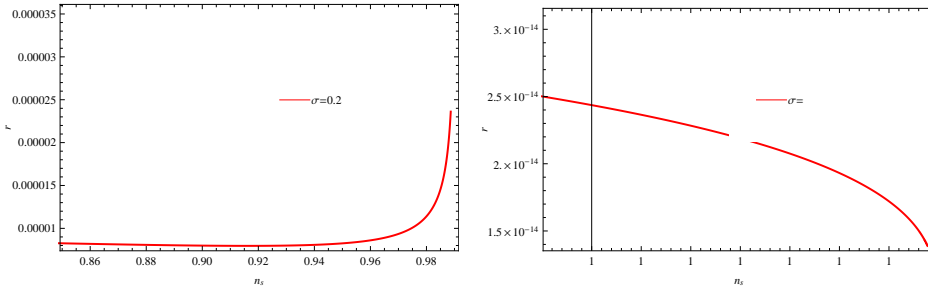


Figure 9: Plot of r versus n_s for MCG model in weak (left panel) and strong (right panel) dissipative regimes for positive potential with $n = -2$.

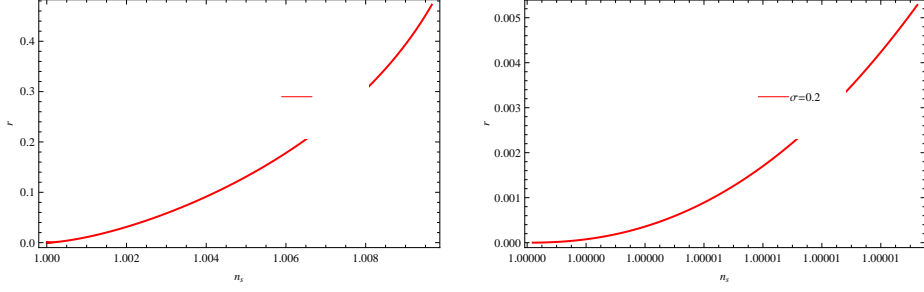


Figure 10: Plot of r versus n_s for MCG model in weak (left panel) and strong (right panel) dissipative regimes for negative potential with $n = 1$.

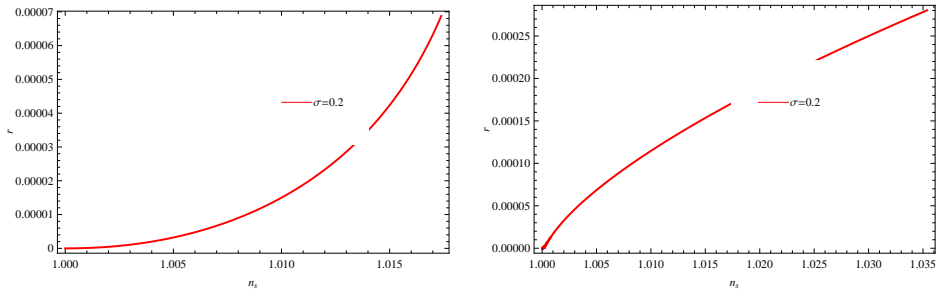


Figure 11: Plot of r versus n_s for MCG model in weak (left panel) and strong (right panel) dissipative regimes for negative potential with $n = -1$.

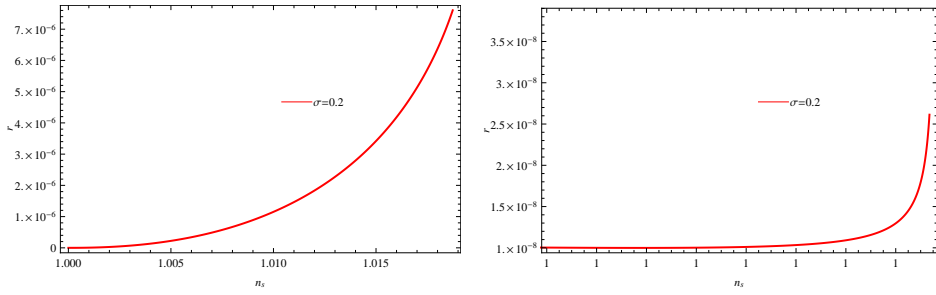


Figure 12: Plot of r versus n_s for MCG model in weak (left panel) and strong (right panel) dissipative regimes for negative potential with $n = -2$.

5 Generalized Cosmic Chaplygin Gas

This model is introduced by Gonzalez-Diaz [60] and its EoS is

$$\rho_{gccg} = -\rho^{-\alpha} (C_5 + (\rho_{gccg}^{1+\alpha} - C_5)^{-\delta}). \quad (35)$$

Here, $C_5 = \frac{D}{1+\delta} - 1$, D takes positive or negative value, α is positive constant and $-l < \delta < 0$, $l > 1$. In the limiting case $\delta \rightarrow 0$, GCCG reduces to GCG. For GCCG model, the energy density has the following form

$$\rho_{gccg} = \left(C_5 + \left(1 + \frac{C_6}{a^{3(1+\alpha)(1+\delta)}} \right)^{\frac{1}{1+\delta}} \right)^{\frac{1}{1+\alpha}}. \quad (36)$$

The corresponding Friedmann equation becomes

$$H^2 = \frac{1}{3M_p^2} \left((C_5 + (1 + \rho_\phi^{(1+\alpha)(1+\delta)})^{\frac{1}{1+\delta}})^{\frac{1}{1+\alpha}} + \rho_\gamma \right). \quad (37)$$

Under certain assumptions, the above Friedmann equation takes the following form

$$H^2 \sim \frac{1}{3M_p^2} \left(C_5 + (1 + V^{(1+\alpha)(1+\delta)})^{\frac{1}{1+\delta}} \right)^{\frac{1}{1+\alpha}}. \quad (38)$$

5.1 Weak Dissipative Regime

The temperature remain same as in both above cases but the slow-roll parameters in this case take the form

$$\begin{aligned} \epsilon &= \frac{M_p^2 V^{(1+\alpha)(1+\delta)-1} (1 + V^{(1+\alpha)(1+\delta)})^{\frac{-\delta}{1+\delta}} V'^2}{2(C_5 + (1 + V^{(1+\alpha)(1+\delta)})^{\frac{1}{1+\delta}})^{\frac{2+\alpha}{1+\alpha}}}, \\ \eta &= \frac{M_p^2}{(C_5 + (1 + V^{(1+\alpha)(1+\delta)})^{\frac{1}{1+\delta}})^{\frac{1}{1+\alpha}}} (2V'' \\ &+ \frac{V'^2((1+\alpha)(1+\delta)-1)}{V} - \frac{\delta(1+\alpha)V^{(1+\alpha)(1+\delta)-1}V'^2}{(1 + V^{(1+\alpha)(1+\delta)})} \\ &- \frac{(1 + V^{(1+\alpha)(1+\delta)})^{\frac{-\delta}{1+\delta}} V'^2}{(C_5 + (1 + V^{(1+\alpha)(1+\delta)})^{\frac{1}{1+\delta}})^{\frac{1}{1+\delta}}} (1 + \alpha)V^{(1+\alpha)(1+\delta)-1}), \\ \beta &= M_p^2 \left(2(C_5 + (1 + V^{(1+\alpha)(1+\delta)})^{\frac{1}{1+\delta}})^{\frac{1}{1+\alpha}} (2n V'' - n V'(n-1)\phi^{-1} \right. \end{aligned}$$

$$\begin{aligned}
& - V'(4-n)(n-1)\phi^{-1} - 3n V'^2 V^{(1+\alpha)(1+\delta)-1} (1 + V^{(1+\alpha)(1+\delta)})^{\frac{-\delta}{1+\delta}} \\
& \times \left(2(4-n)(C_5 + (1 + V^{(1+\alpha)(1+\delta)})^{\frac{1}{1+\delta}})^{\frac{2+\alpha}{1+\alpha}} \right)^{-1} \Big). \tag{39}
\end{aligned}$$

Taking into account Eq.(8), the relation for number of e-folds becomes

$$N = \frac{1}{M_P^2} \int_{\phi_{end}}^{\phi_*} \frac{(C_5 + (1 + V^{(1+\alpha)(1+\delta)})^{\frac{1}{1+\delta}})^{\frac{1}{1+\alpha}}}{V'} d\phi.$$

For this model, the power spectrum, scalar spectral index and tensor-to-scalar ratio in the form of potential can be found by using Eq.(9)-(11) as follow

$$\begin{aligned}
\mathcal{P}_{\mathcal{R}} &= \left(\frac{81\pi}{4} \right)^{\frac{1}{2}} \frac{\left(C_5 + (1 + V^{(1+\alpha)(1+\delta)})^{\frac{1}{1+\delta}} \right)^{\frac{(15-6n)}{2(1+\alpha)(4-n)}} c^{\frac{3}{4-n}}}{3^{\frac{15-6n}{2(4-n)}} M_p^{\frac{15-6n}{4-n}} V'^{\frac{6-3n}{4-n}} 6^{\frac{n+2}{4-n}} c_*^{\frac{n+2}{2(4-n)}} \phi^{\frac{(n-1)(4-n)-(n-1)(n+2)}{2(4-n)}}} \tag{40} \\
n_s - 1 &= \frac{3M_p^2}{2(C_5 + (1 + V^{(1+\alpha)(1+\delta)})^{\frac{1}{1+\delta}})^{1+\alpha}} \left(\frac{V'^2((1+\alpha)(1+\delta) - 1)}{V} \right. \\
& - (3 \left(2(C_5 + (1 + V^{(1+\alpha)(1+\delta)})^{\frac{1}{1+\delta}}) (2n V'' - n V'(n-1)\phi^{-1} \right. \\
& - V'(4-n)(n-1)\phi^{-1} - 3n V'^2 V^{(1+\alpha)(1+\delta)-1} (1 + V^{(1+\alpha)(1+\delta)})^{\frac{-\delta}{1+\delta}} \\
& \times \left. \left. \left(2(2)(4-n)(C_5 + (1 + V^{(1+\alpha)(1+\delta)})^{\frac{1}{1+\delta}}) \right)^{-1} + 2V'' - \delta(1+\alpha) \right. \right. \\
& \times V^{(1+\alpha)(1+\delta)-1} V'^2 \left((1 + V^{(1+\alpha)(1+\delta)}) \right)^{-1} - \left. \left. \left(1 + V^{(1+\alpha)(1+\delta)} \right)^{\frac{-\delta}{1+\delta}} \right. \right. \\
& \times V'^2(1+\alpha) V^{(1+\alpha)(1+\delta)-1} \left(C_5 + (1 + V^{(1+\alpha)(1+\delta)})^{\frac{1}{1+\delta}} \right)^{-1} \\
& \times \left. \left. \left(\frac{3}{4} + (1+\alpha) \right) \right) \right), \tag{41}
\end{aligned}$$

$$r = \frac{32G V'^{\frac{6-3n}{4-n}} \phi^{\frac{(n-1)(4-n)+(n-1)(n+2)}{2(4-n)}} 6^{\frac{n+2}{4-n}} c_*^{\frac{n+2}{2(4-n)}} 3^{\frac{7-4n}{2(4-n)}} M_p^{\frac{7-4n}{4-n}}}{9c^{\frac{3}{4-n}} \pi^{\frac{3}{2}} \left(C_5 + (1 + V^{(1+\alpha)(1+\delta)})^{\frac{1}{1+\delta}} \right)^{\frac{1}{2(4-n)(1+\alpha)}}}. \tag{42}$$

For positive quadratic and quartic potential, the relations of r and n_s in

terms of scalar field can be expressed as

$$\begin{aligned}
r &= \frac{32G(\sigma^2\phi + \lambda_*\phi^3)^{\frac{6-3n}{4-n}} \phi^{\frac{(n-1)(4-n)+(n-1)(n+2)}{2(4-n)}} 6^{\frac{n+2}{4-n}} c_*^{\frac{n+2}{2(4-n)}} 3^{\frac{7-4n}{2(4-n)}} M_p^{\frac{7-4n}{4-n}}}{9c^{\frac{3}{4-n}} \pi^{\frac{3}{2}} \left(C_5 + \left(1 + \left(\frac{1}{2}\sigma^2\phi^2 + \frac{\lambda_*}{4}\phi^4 \right)^{(1+\alpha)(1+\delta)} \right)^{\frac{1}{1+\delta}} \right)^{\frac{7-4n}{2(4-n)(1+\alpha)}}} \quad (43) \\
n_s - 1 &= \frac{3M_p^2}{2(C_5 + (1 + (\frac{1}{2}\sigma^2\phi^2 + \frac{\lambda_*}{4}\phi^4)^{(1+\alpha)(1+\delta)})^{\frac{1}{1+\delta}})^{1+\alpha}} \\
&\times \left((\sigma^2\phi + \lambda_*\phi^3)^2((1+\alpha)(1+\delta) - 1) \left(\left(\frac{1}{2}\sigma^2\phi^2 + \frac{\lambda_*}{4}\phi^4 \right)^{(1+\alpha)(1+\delta)} \right)^{\frac{1}{1+\delta}} \right. \\
&+ \left. \left(\frac{\lambda_*}{4}\phi^4 \right)^{-1} - \left(3 \left(2 \left(C_5 + \left(1 + \left(\frac{1}{2}\sigma^2\phi^2 + \frac{\lambda_*}{4}\phi^4 \right)^{(1+\alpha)(1+\delta)} \right)^{\frac{1}{1+\delta}} \right) \right. \right. \right. \\
&\times \left. \left. \left. \left(2n \left(\sigma^2 + 3\lambda_*\phi^2 \right) - n(\sigma^2\phi + \lambda_*\phi^3)(n-1)\phi^{-1} - (\sigma^2\phi + \lambda_*\phi^3)(4-n)(n-1)\phi^{-1} \right) \right. \right. \right. \\
&- \left. \left. \left. 3n(\sigma^2\phi + \lambda_*\phi^3)^2 \left(\frac{1}{2}\sigma^2\phi^2 + \frac{\lambda_*}{4}\phi^4 \right)^{(1+\alpha)(1+\delta)-1} \right) \right) \right) / \left(2(2)(4-n) \right) \\
&\times \left(C_5 + \left(1 + \left(\frac{1}{2}\sigma^2\phi^2 + \frac{\lambda_*}{4}\phi^4 \right)^{(1+\alpha)(1+\delta)} \right)^{\frac{1}{1+\delta}} \right) \\
&+ 2(\sigma^2 + 3\lambda_*\phi^2) - \delta(1+\alpha) \left(\frac{1}{2}\sigma^2\phi^2 + \frac{\lambda_*}{4}\phi^4 \right)^{(1+\alpha)(1+\delta)-1} \\
&\times (\sigma^2\phi + \lambda_*\phi^3)^2 \left(\left(1 + \left(\frac{1}{2}\sigma^2\phi^2 + \frac{\lambda_*}{4}\phi^4 \right)^{(1+\alpha)(1+\delta)} \right)^{\frac{1}{1+\delta}} \right)^{-1} \\
&- \left(1 + \left(\frac{1}{2}\sigma^2\phi^2 + \frac{\lambda_*}{4}\phi^4 \right)^{(1+\alpha)(1+\delta)} \right)^{\frac{-\delta}{1+\delta}} (\sigma^2\phi + \lambda_*\phi^3)^2 \\
&\times (1+\alpha) \left(\frac{1}{2}\sigma^2\phi^2 + \frac{\lambda_*}{4}\phi^4 \right)^{(1+\alpha)(1+\delta)-1} \left(C_5 + \left(1 + \left(\frac{1}{2}\sigma^2\phi^2 + \frac{\lambda_*}{4}\phi^4 \right)^{(1+\alpha)(1+\delta)} \right)^{\frac{1}{1+\delta}} \right)^{-1} \\
&+ \left. \left(\frac{3}{4} + (1+\alpha) \right) \right). \quad (44)
\end{aligned}$$

For negative quadratic and quartic potential, the relations of r and n_s in

terms of scalar field are given by

$$\begin{aligned}
r &= \frac{32G(-\sigma^2\phi + \lambda_*\phi^3)^{\frac{6-3n}{4-n}} \phi^{\frac{(n-1)(4-n)+(n-1)(n+2)}{2(4-n)}} 6^{\frac{n+2}{4-n}} c_*^{\frac{n+2}{2(4-n)}} 3^{\frac{7-4n}{2(4-n)}} M_p^{\frac{7-4n}{4-n}}}{9c^{\frac{3}{4-n}} \pi^{\frac{3}{2}} \left(C_5 + \left(1 + \left(s - \frac{1}{2}\sigma^2\phi^2 + \frac{\lambda_*}{4}\phi^4 \right)^{(1+\alpha)(1+\delta)} \right)^{\frac{1}{1+\delta}} \right)^{\frac{7-4n}{2(4-n)(1+\alpha)}}} \quad (45) \\
n_s - 1 &= \frac{3M_p^2}{2 \left(C_5 + \left(1 + \left(s - \frac{1}{2}\sigma^2\phi^2 + \frac{\lambda_*}{4}\phi^4 \right)^{(1+\alpha)(1+\delta)} \right)^{\frac{1}{1+\delta}} \right)^{1+\alpha}} \\
&\times \left(\frac{(-\sigma^2\phi + \lambda_*\phi^3)^2((1+\alpha)(1+\delta) - 1)}{(s - \frac{1}{2}\sigma^2\phi^2 + \frac{\lambda_*}{4}\phi^4)} - \left(3 \left(2 \left(C_5 \right. \right. \right. \right. \\
&+ \left. \left. \left(1 + \left(s - \frac{1}{2}\sigma^2\phi^2 + \frac{\lambda_*}{4}\phi^4 \right)^{(1+\alpha)(1+\delta)} \right)^{\frac{1}{1+\delta}} \right) \left(2n(\right. \right. \\
&- \sigma^2 + 3\lambda_*\phi^2) - n(-\sigma^2\phi + \lambda_*\phi^3)(n-1)\phi^{-1} - (\\
&- \sigma^2\phi + \lambda_*\phi^3)(4-n)(n-1)\phi^{-1} \Big) - 3n(-\sigma^2\phi \\
&+ \lambda_*\phi^3)^2(s - \frac{1}{2}\sigma^2\phi^2 + \frac{\lambda_*}{4}\phi^4)^{(1+\alpha)(1+\delta)-1} \left(1 + \left(s - \frac{1}{2} \right. \right. \\
&\times \left. \left. \sigma^2\phi^2 + \frac{\lambda_*}{4}\phi^4 \right)^{(1+\alpha)(1+\delta)} \right)^{\frac{-\delta}{1+\delta}} \Big) \Big) / \left(2(2)(4-n) \left(C_5 \right. \right. \\
&+ \left. \left(1 + \left(s - \frac{1}{2}\sigma^2\phi^2 + \frac{\lambda_*}{4}\phi^4 \right)^{(1+\alpha)(1+\delta)} \right)^{\frac{1}{1+\delta}} \right) \Big) + 2(-\sigma^2 + 3\lambda_*\phi^2) \\
&- \frac{\delta(1+\delta)(s - \frac{1}{2}\sigma^2\phi^2 + \frac{\lambda_*}{4}\phi^4)^{(1+\alpha)(1+\delta)-1}(-\sigma^2\phi + \lambda_*\phi^3)^2}{\left(1 + \left(s - \frac{1}{2}\sigma^2\phi^2 + \frac{\lambda_*}{4}\phi^4 \right)^{(1+\alpha)(1+\delta)} \right)} \\
&- \left(1 + \left(s - \frac{1}{2}\sigma^2\phi^2 + \frac{\lambda_*}{4}\phi^4 \right)^{(1+\alpha)(1+\delta)} \right)^{\frac{-\delta}{1+\delta}} (-\sigma^2\phi + \lambda_*\phi^3)^2(1+\alpha) \\
&\times \left(s - \frac{1}{2}\sigma^2\phi^2 + \frac{\lambda_*}{4}\phi^4 \right)^{(1+\alpha)(1+\delta)-1} \left(\left(C_5 + \left(1 + \left(s - \frac{1}{2}\sigma^2\phi^2 \right. \right. \right. \right. \\
&+ \left. \left. \frac{\lambda_*}{4}\phi^4 \right)^{(1+\alpha)(1+\delta)} \right)^{\frac{1}{1+\delta}} \Big) \Big)^{-1} \left(\frac{3}{4} + (1+\alpha) \right) \Big) \Big). \quad (46)
\end{aligned}$$

5.2 Strong Dissipative Regime

In this case, the slow roll parameters become

$$\begin{aligned}
\epsilon &= \frac{M_p^2 V^{(1+\alpha)(1+\delta)-1} (1 + V^{(1+\alpha)(1+\delta)})^{\frac{-\delta}{1+\delta}} V'^2}{2R(C_5 + (1 + V^{(1+\alpha)(1+\delta)})^{\frac{1}{1+\delta}})^{\frac{2+\alpha}{1+\alpha}}}, \\
\eta &= \frac{M_p^2}{R(C_5 + (1 + V^{(1+\alpha)(1+\delta)})^{\frac{1}{1+\delta}})^{\frac{1}{1+\delta}}} (2V'' + \frac{V'^2((1+\alpha)(1+\delta)-1)}{V} \\
&\quad - \frac{\delta(1+\alpha)V^{(1+\alpha)(1+\delta)-1}V'^2}{(1 + V^{(1+\alpha)(1+\delta)})} - \frac{(1 + V^{(1+\alpha)(1+\delta)})^{\frac{-\delta}{1+\delta}}V'^2}{(C_5 + (1 + V^{(1+\alpha)(1+\delta)})^{\frac{1}{1+\delta}})} \\
&\quad \times (1+\alpha)V^{(1+\alpha)(1+\delta)-1}), \\
\beta &= n M_p^2 \left(4V''(C_5 + (1 + V^{(1+\alpha)(1+\delta)})^{\frac{1}{1+\delta}}) - ((1 + V^{(1+\alpha)(1+\delta)})^{\frac{-\delta}{1+\delta}}V'^2 V^{(1+\alpha)(1+\delta)-1}) \right) (2R(n+4) \\
&\quad \times (C_5 + (1 + V^{(1+\alpha)(1+\delta)})^{\frac{1}{1+\delta}})^{\frac{2+\alpha}{1+\alpha}})^{-1}. \tag{47}
\end{aligned}$$

The expression of number of e-folds is given by

$$N = \frac{1}{M_P^2} \int_{\phi_{end}}^{\phi_*} \frac{(C_5 + (1 + V^{(1+\alpha)(1+\delta)})^{\frac{1}{1+\delta}})^{\frac{1}{1+\alpha}}}{V'} R d\phi.$$

The perturbation quantities turn out to be

$$\begin{aligned}
\mathcal{P}_{\mathcal{R}} &= \left(\frac{\pi}{4}\right)^{\frac{1}{2}} \frac{\left(C_5 + (1 + V^{(1+\alpha)(1+\delta)})^{\frac{1}{1+\delta}}\right)^{\frac{9}{2(1+\alpha)(n+4)}} c^{\frac{9}{n+4}}}{3^{\frac{9}{2(n+4)}} M_p^{\frac{9}{n+4}} (4C_*)^{\frac{5n+2}{2(n+4)}} \phi^{\frac{5(n-1)(n+4)-(n-1)(5n+2)}{2(n+4)}} V'^{\frac{6-3n}{n+4}}}, \\
r &= \frac{32G V'^{\frac{8-5n}{5}} \phi^{\frac{5(n-1)}{2}} (4C_*)^{\frac{5n+2}{10}} (C_5 + (1 + V^{(1+\alpha)(1+\delta)}))^{\frac{5n-3}{20(1+\alpha)}}}{c^{\frac{23-5n}{10}} \pi^{\frac{3}{2}} 3^{\frac{5n-3}{20}} M_p^{\frac{5n-3}{10}}}, \\
n_s - 1 &= \frac{3M_p^{\frac{4}{n+4}} 3^{\frac{2}{n+4}} (4C_*)^{\frac{n}{n+4}} \phi^{\frac{(n+4)(n-1)-n(n-1)}{n+4}}}{2c^{\frac{4}{n+4}} V'^{\frac{2n}{n+4}} (C_5 + (1 + V^{(1+\alpha)(1+\delta)})^{\frac{1}{1+\delta}})^{\frac{2}{(n+4)(1+\alpha)}}} \\
&\quad \times \left(\frac{V'^2((1+\alpha)(1+\delta)-1)}{V} - 3n \left(4V''(C_5 + (1 + V^{(1+\alpha)(1+\delta)})^{\frac{1}{1+\delta}}) \right) \right)
\end{aligned}$$

$$\begin{aligned}
& - \left(1 + V^{(1+\alpha)(1+\delta)}\right)^{\frac{-\delta}{1+\delta}} V'^2 V^{(1+\alpha)(1+\delta)-1} \Bigg) (4(n+4)(C_5 + (1 \\
& + V^{(1+\alpha)(1+\delta)})^{\frac{1}{1+\delta}}))^{-1} + 2V'' - \frac{\delta(1+\alpha)V^{(1+\alpha)(1+\delta)-1}V'^2}{(1 + V^{(1+\alpha)(1+\delta)})} \\
& - \frac{(1 + V^{(1+\alpha)(1+\delta)})^{\frac{-\delta}{1+\delta}} V'^2 (1 + \alpha) V^{(1+\alpha)(1+\delta)-1}}{(C_5 + (1 + V^{(1+\alpha)(1+\delta)})^{\frac{1}{1+\delta}})} \left(\frac{3}{4} \right. \\
& \left. + (1 + \alpha) \right) \Bigg). \tag{48}
\end{aligned}$$

For positive quadratic and quartic potential, the tensor-to-scalar ratio and scalar spectral index in terms of ϕ can be expressed as follows

$$\begin{aligned}
r &= 32G(\sigma^2\phi + \lambda_*\phi^3)^{\frac{8-5n}{5}} \phi^{\frac{5(n-1)}{2}} (4C_*)^{\frac{5n+2}{10}} \left(C_5 + \left(1 + \left(\frac{1}{2}\sigma^2\phi^2 + \frac{\lambda_*}{4}\phi^4 \right)^{(1+\alpha)(1+\delta)} \right)^{\frac{5n-3}{20(1+\alpha)}} \left(c^{\frac{23-5n}{10}} \pi^{\frac{3}{2}} 3^{\frac{5n-3}{20}} M_p^{\frac{5n-3}{10}} \right)^{-1}, \right. \\
n_s - 1 &= 3M_p^{\frac{4}{n+4}} 3^{\frac{2}{n+4}} (4C_*)^{\frac{n}{n+4}} \phi^{\frac{(n+4)(n-1)-n(n-1)}{n+4}} (2c^{\frac{4}{n+4}} (\sigma^2\phi + \lambda_*\phi^3)^{\frac{2n}{n+4}} (C_5 + (1 + (\frac{1}{2}\sigma^2\phi^2 + \frac{\lambda_*}{4}\phi^4)^{(1+\alpha)(1+\delta)})^{\frac{1}{1+\delta}})^{\frac{2}{(n+4)(1+\alpha)}})^{-1} \\
& \times \left(\frac{(\sigma^2\phi + \lambda_*\phi^3)^2((1+\alpha)(1+\delta)-1)}{(\frac{1}{2}\sigma^2\phi^2 + \frac{\lambda_*}{4}\phi^4)} - 3n(4(\sigma^2 + 3\lambda_*\phi^2)) \right. \\
& \times (C_5 + (1 + (\frac{1}{2}\sigma^2\phi^2 + \frac{\lambda_*}{4}\phi^4)^{(1+\alpha)(1+\delta)})^{\frac{1}{1+\delta}}) - (1 + (\frac{1}{2}\sigma^2\phi^2 + \frac{\lambda_*}{4}\phi^4)^{(1+\alpha)(1+\delta)})^{\frac{-\delta}{1+\delta}} (\sigma^2\phi + \lambda_*\phi^3)^2 (\frac{1}{2}\sigma^2\phi^2 + \frac{\lambda_*}{4}\phi^4)^{(1+\alpha)(1+\delta)-1} \\
& \times (4(n+4)(C_5 + (1 + (\frac{1}{2}\sigma^2\phi^2 + \frac{\lambda_*}{4}\phi^4)^{(1+\alpha)(1+\delta)})^{\frac{1}{1+\delta}}))^{-1} + 2 \\
& \times (\sigma^2 + 3\lambda_*\phi^2) - \frac{\delta(\frac{1}{2}\sigma^2\phi^2 + \frac{\lambda_*}{4}\phi^4)^{(1+\alpha)(1+\delta)-1}(\sigma^2\phi + \lambda_*\phi^3)^2}{(1+\alpha)^{-1}(1 + (\frac{1}{2}\sigma^2\phi^2 + \frac{\lambda_*}{4}\phi^4)^{(1+\alpha)(1+\delta)})} \\
& - (1 + (\frac{1}{2}\sigma^2\phi^2 + \frac{\lambda_*}{4}\phi^4)^{(1+\alpha)(1+\delta)})^{\frac{-\delta}{1+\delta}} (\sigma^2\phi + \lambda_*\phi^3)^2 (1 + \alpha) \\
& \times (\frac{1}{2}\sigma^2\phi^2 + \frac{\lambda_*}{4}\phi^4)^{(1+\alpha)(1+\delta)-1} ((C_5 + (1 + (\frac{1}{2}\sigma^2\phi^2 + \frac{\lambda_*}{4}\phi^4)^{(1+\alpha)(1+\delta)})^{\frac{1}{1+\delta}})^{-1} + (1 + \alpha)) \\
& \times \left. \right) \left(\frac{3}{4} + (1 + \alpha) \right) \Bigg). \tag{49}
\end{aligned}$$

For negative quadratic and quartic potential, the tensor to scalar ratio and scalar spectral index in terms of ϕ can be obtained as

$$\begin{aligned}
r &= 32G(-\sigma^2\phi + \lambda_*\phi^3)^{\frac{8-5n}{5}}\phi^{\frac{5(n-1)}{2}}(4C_*)^{\frac{5n+2}{10}}(C_5 + (1 + (s - \frac{1}{2}\sigma^2\phi^2 \\
&+ \frac{\lambda_*}{4}\phi^4)^{(1+\alpha)(1+\delta)}))^{\frac{5n-3}{20(1+\alpha)}}(c^{\frac{23-5n}{10}}\pi^{\frac{3}{2}}3^{\frac{5n-3}{20}}M_p^{\frac{5n-3}{10}})^{-1}, \\
n_s - 1 &= 3M_p^{\frac{4}{n+4}}3^{\frac{2}{n+4}}(4C_*)^{\frac{n}{n+4}}\phi^{\frac{(n+4)(n-1)-n(n-1)}{n+4}}(2c^{\frac{4}{n+4}}(-\sigma^2\phi + \lambda_*\phi^3 \\
&\times)^{\frac{2n}{n+4}}(C_5 + (1 + (s - \frac{1}{2}\sigma^2\phi^2 + \frac{\lambda_*}{4}\phi^4)^{(1+\alpha)(1+\delta)})^{\frac{1}{1+\delta}})^{\frac{2}{(n+4)(1+\alpha)}})^{-1} \\
&\times \left(\frac{(-\sigma^2\phi + \lambda_*\phi^3)^2((1+\alpha)(1+\delta) - 1)}{(s - \frac{1}{2}\sigma^2\phi^2 + \frac{\lambda_*}{4}\phi^4)} - 3n \left(4(-\sigma^2 + 3\lambda_*\phi^2) \right. \right. \\
&\times (C_5 + (1 + (s - \frac{1}{2}\sigma^2\phi^2 + \frac{\lambda_*}{4}\phi^4)^{(1+\alpha)(1+\delta)})^{\frac{1}{1+\delta}}) - (1 + (s - \frac{1}{2} \\
&\times \sigma^2\phi^2 + \frac{\lambda_*}{4}\phi^4)^{(1+\alpha)(1+\delta)})^{\frac{-\delta}{1+\delta}}(-\sigma^2\phi + \lambda_*\phi^3)^2(s - \frac{1}{2}\sigma^2\phi^2 + \frac{\lambda_*}{4}\phi^4 \\
&\times)^{(1+\alpha)(1+\delta)-1})(4(n+4)(C_5 + (1 + (s - \frac{1}{2}\sigma^2\phi^2 + \frac{\lambda_*}{4}\phi^4 \\
&\times)^{(1+\alpha)(1+\delta)})^{\frac{1}{1+\delta}}))^{\frac{1}{1+\delta}})^{-1} + 2(-\sigma^2 + 3\lambda_*\phi^2) - \delta(1+\alpha)(s - \frac{1}{2}\sigma^2\phi^2 \\
&+ \frac{\lambda_*}{4}\phi^4)^{(1+\alpha)(1+\delta)-1}(-\sigma^2\phi + \lambda_*\phi^3)^2((1 + (s - \frac{1}{2}\sigma^2\phi^2 + \frac{\lambda_*}{4}\phi^4 \\
&\times)^{(1+\alpha)(1+\delta)}))^{\frac{-\delta}{1+\delta}}(-\sigma^2 \\
&\times \phi + \lambda_*\phi^3)^2(1+\alpha)(s - \frac{1}{2}\sigma^2\phi^2 + \frac{\lambda_*}{4}\phi^4)^{(1+\alpha)(1+\delta)-1}((C_5 + (1 + (s \\
&- \frac{1}{2}\sigma^2\phi^2 + \frac{\lambda_*}{4}\phi^4)^{(1+\alpha)(1+\delta)})^{\frac{1}{1+\delta}}))^{\frac{1}{1+\delta}})^{-1}(\frac{3}{4} + (1+\alpha)) \Bigg). \quad (50)
\end{aligned}$$

For GCCG model, the plots of r and n_s for weak/strong dissipative regimes for both positive/negative quadratic and quartic potential for three different values of $n = 1, -1, -2$, respectively are shown in Figures **13-18**. The observed constraints of scalar ratio and spectral index are displayed in the Tables **3(a)** and **3(b)**. It is found that the results are compatible with WMAP9 [57] and Planck 2015 [58].

Table 3(a): GCCG Weak and Strong Dissipative Regime with Positive Quadratic and Quartic Potential.

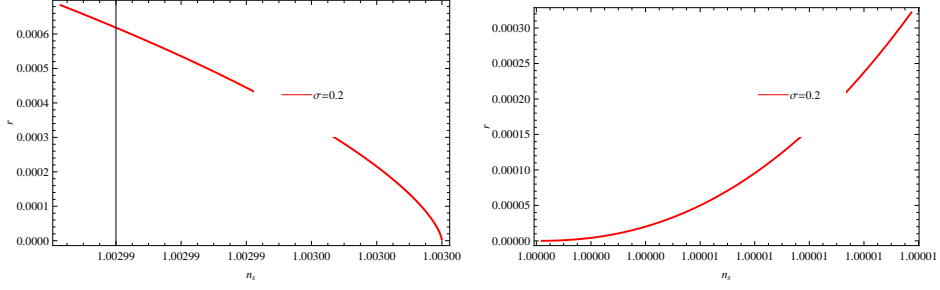


Figure 13: Plot of r versus n_s for GCCG model in weak (left panel) and strong (right panel) dissipative regimes for positive potential with $n = 1$.

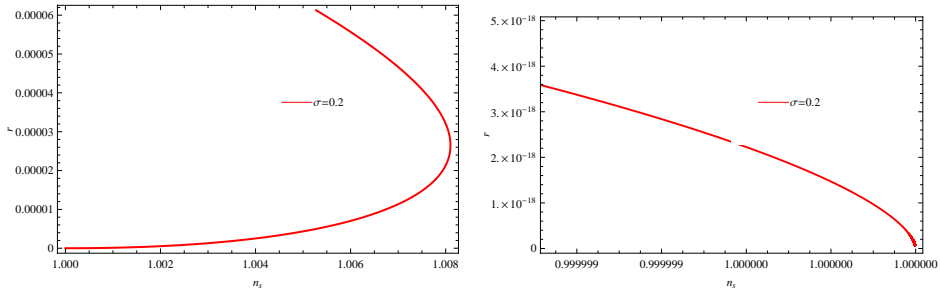


Figure 14: Plot of r versus n_s for GCCG model in weak (left panel) and strong (right panel) dissipative regimes for positive potential with $n = -1$.

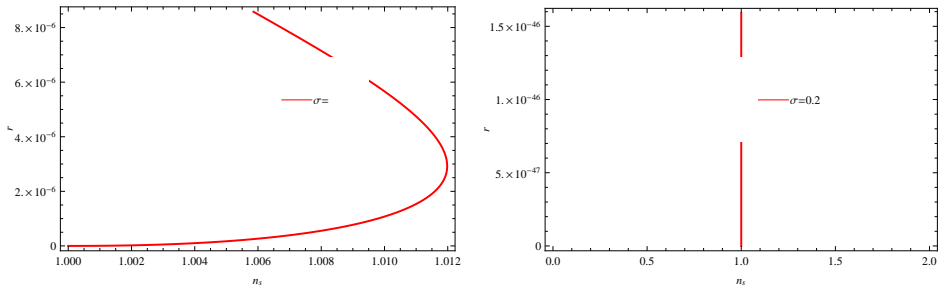


Figure 15: Plot of r versus n_s for GCCG model in weak (left panel) and strong (right panel) dissipative regimes for positive potential with $n = -2$.

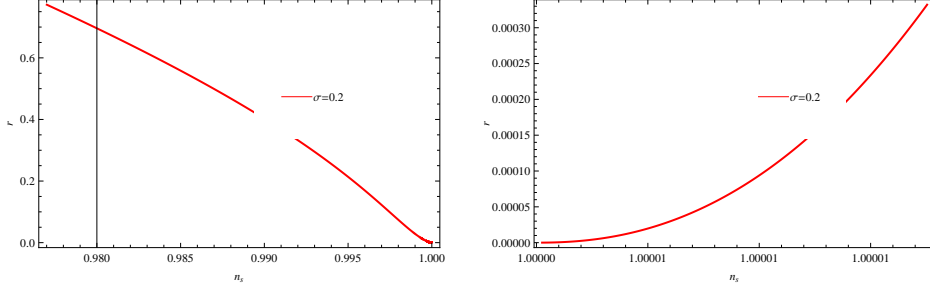


Figure 16: Plot of r versus n_s for GCCG model in weak (left panel) and strong (right panel) dissipative regimes for negative potential with $n = 1$.

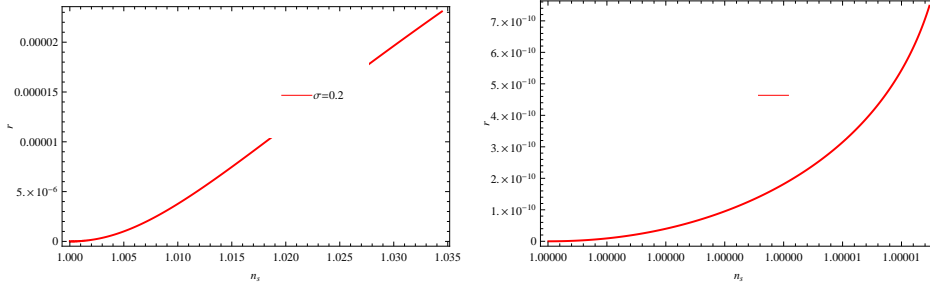


Figure 17: Plot of r versus n_s for GCCG model in weak (left panel) and strong (right panel) dissipative regimes for negative potential with $n = -1$.

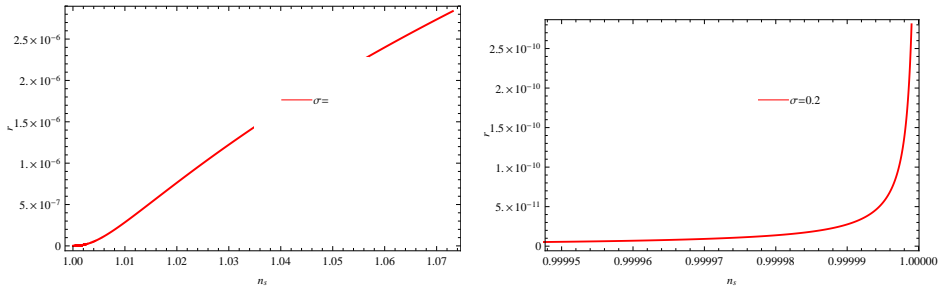


Figure 18: Plot of r versus n_s for GCCG model in weak (left panel) and strong (right panel) dissipative regimes for negative potential with $n = -2$.

<i>Sr.No</i>	<i>n</i>	<i>r</i> (<i>W</i>)	<i>n_s</i> (<i>W</i>)	<i>r</i> (<i>S</i>)	<i>n_s</i> (<i>S</i>)
1	1	≤ 0.0007	$1.0029^{+0.001}_{-0.001}$	≤ 0.00032	$1.0000^{+0.0001}_{-0.0001}$
2	-1	≤ 0.000062	$1.004^{+0.001}_{-0.001}$	$\leq 3.5 \times 10^{-18}$	$1.000^{+0.001}_{-0.0001}$
3	-2	$\leq 8.2 \times 10^{-6}$	$1.011^{+0.001}_{-0.001}$	$\leq 1.5 \times 10^{-46}$	$0.9^{+0.1}_{-0.1}$

Table 3(b): GCCG Weak and Strong Dissipative Regime with Negative Quadratic and Quartic Potential.

<i>sr.No</i>	<i>n</i>	<i>r</i> (<i>W</i>)	<i>n_s</i> (<i>W</i>)	<i>r</i> (<i>S</i>)	<i>n_s</i> (<i>S</i>)
1	1	≤ 0.8	$0.999^{+0.001}_{-0.001}$	≤ 0.00033	$1.0000^{+0.0001}_{-0.0001}$
2	-1	≤ 0.000025	$1.034^{+0.001}_{-0.001}$	$\leq 7.2 \times 10^{-10}$	$1.0000^{+0.0001}_{-0.0001}$
3	-2	$\leq 2.7 \times 10^{-6}$	$1.06^{+0.001}_{-0.001}$	$\leq 2.7 \times 10^{-10}$	$1.0000^{+0.0001}_{-0.0001}$

6 Concluding Remarks

We have studied warm polynomial inflation (with positive/negative quadratic and quartic potentials) by assuming generalized form of dissipative coefficient ($\Gamma = c \frac{T^n}{\phi^{n-1}}$). In order to get the consistency of the results, we have considered different CG models like GCG, MCG, and GCCG. We have calculated inflationary parameters for both weak and strong dissipative regimes such as number of e-folds, scalar spectrum, scalar spectral index and tensor to scalar ratio. For clear analysis of results, we have displayed the trajectories between tensor-to-scalar ratio (*r*) and spectral index (*n_s*) in weak and strong dissipative regimes for all CG models. The obtain results for all CG models in the form of upper bounds of *r* and *n_s* are summarized below:

GCG model:

- For positive quadratic and quartic potential, $r \leq 0.0104168$, 1.2×10^{-6} , 1.4×10^{-14} with respect to $n_s = 0.98^{+0.01}_{-0.01}$, $0.96^{+0.02}_{-0.02}$, $1.00001^{+0.00001}_{-0.00001}$, respectively, for $n = 1, -1, -2$ in weak dissipative regime. However, for strong dissipative regime, $r \leq 0.06$, 3.0×10^{-15} , 3.7×10^{-43} for $n_s = 0.90^{+0.06}_{-0.06}$, $0.94^{+0.02}_{-0.02}$, $1.00011^{+0.00001}_{-0.00001}$ respectively.

- For negative quadratic and quartic potential, the results of tensor-to-scalar ratio and scalar spectral index in weak dissipative regime are $r \leq 0.38, 0.000041, 4.5 \times 10^{-6}$ according to $n_s = 1.0000^{+0.0001}_{-0.0001}, 1.0031^{+0.0001}_{-0.0001}, 1.0040^{+0.0001}_{-0.0001}$ respectively, and for strong dissipative regime $r \leq 0.0055, 4.0 \times 10^{-28}, 5.2 \times 10^{-44}$ for $n_s = 1.0004^{+0.0001}_{-0.0001}, 1.000057^{+0.000001}_{-0.000001}, 1.00002^{+0.00001}_{-0.00001}$ respectively.

MCG model:

- For positive quadratic and quartic potential, $r \leq 0.005, 0.05, 0.000025$ according to $n_s = 1.00001^{+0.00001}_{-0.00001}, 1.17^{+0.001}_{-0.001}, 0.98^{+0.01}_{-0.011}$, respectively. Similarly, for strong dissipative regime, the results are $r \leq 0.00025, 0.00028, 2.5 \times 10^{-14}$ for $n_s = 1.0000^{+0.0001}_{-0.0001}, 1.034^{+0.001}_{-0.001}, 0.9^{+0.1}_{-0.1}$.
- The results with negative quadratic and quartic potential are $r \leq 0.5, 0.00007, 7.2 \times 10^{-6}$ for $n_s = 1.0009^{+0.0001}_{-0.0001}, 1.019^{+0.001}_{-0.001}, 1.019^{+0.001}_{-0.001}$ and for strong dissipative regime $r \leq 0.0052, 0.00028, 2.5 \times 10^{-8}$ with respect to $n_s = 1.00000^{+0.00001}_{-0.00001}, 1.034^{+0.001}_{-0.001}, 0.9^{+0.1}_{-0.1}$.

GCCG model:

- For positive quadratic and quartic potential, $r \leq 0.0007, 0.000062, 8.2 \times 10^{-6}$ with respect to $n_s = 1.0029^{+0.0001}_{-0.0001}, 1.004^{+0.001}_{-0.001}, 1.011^{+0.001}_{-0.001}$. In the similar way, for strong dissipative regime, the constraints are $r \leq 0.00032, 3.5 \times 10^{-18}, 1.5 \times 10^{-46}$ for $n_s = 1.0000^{+0.0001}_{-0.0001}, 1.000^{+0.001}_{-0.001}, 0.9^{+0.1}_{-0.1}$.
- For negative quadratic and quartic potential, the results for tensor-to-scalar ratio and scalar spectral index in weak dissipative regime are $r \leq 0.8, 0.000025, 2.7 \times 10^{-6}$ for $n_s = 0.999^{+0.001}_{-0.001}, 1.034^{+0.001}_{-0.001}, 1.06^{+0.01}_{-0.01}$, and for strong dissipative regime, the results are $r \leq 0.00033, 7.2 \times 10^{-10}, 2.7 \times 10^{-10}$ for $n_s = 1.0000^{+0.0001}_{-0.0001}, 1.0000^{+0.0001}_{-0.0001}, 1.0000^{+0.0001}_{-0.0001}$ respectively.

It is interesting to mentioned here that the above results of r and n_s lie within the constraints of WMAP9 [57] and Planck 2015 [58] (as mentioned in Table 1).

Acknowledgments

Abdul Jawad is thankful to the Higher Education Commission, Islamabad, Pakistan for its financial support under the grant No: 5412/Federal/NRPU/R&D/HEC/2016 of NATIONAL RESEARCH PROGRAMME FOR UNIVERSITIES (NRPU). N.V. was supported by Comisión Nacional de Ciencias y Tecnología of Chile through FONDECYT Grant N° 3150490. Finally, the authors wish to thank the anonymous referee for her/his valuable comments, which have helped us to improve the presentation in our manuscript.

References

- [1] Ade, P. A. R., et al.: Astron. Astrophys. **A20**, (2016)594.
- [2] Starobinsky, A.A.: Phys. Lett. B **91**(1980); Guth, A.: Phys. Rev. D **23**(1981)347.
- [3] Gold, B. et al.: Astrophys. J. Suppl. **192**(2011)15.
- [4] Liddle, A.R. and Lyth, D.H.: Cosmological Inflation and Large-Scale Structure, Cambridge University Press, Cambridge, U.K.(2000).
- [5] Weinberg, S.: Cosmology, Oxford University Press, Oxford U.K. (2008).
- [6] Dodelson, S.: Modern Cosmology, Academic Press(2008).
- [7] Bassett, B.A., Tsujikawa, S. and Wands, D.: Rev. Mod. Phys. **78** (2006) 537.
- [8] Berera, A.: Phys. Rev. Lett. **75** (1995) 3218.
- [9] Berera, A. and Fang, L.Z.: Phys. Rev. Lett. **74** (1995) 1912.
- [10] Hall, L.M.H., Moss, I.G. and Berera, A.: Phys. Rev. D **69** (2004) 083525.
- [11] Berera, A.: Nucl. Phys. B **585** (2000) 666.
- [12] M. Bastero-Gil and A. Berera, Int. J. Mod. Phys. A **24**, 2207 (2009).
- [13] Linde, A.D.: Phys. Lett. B **129**(1983)177.
- [14] A. Pich, arXiv:0705.4264 [hep-ph].

- [15] P. W. Higgs, Phys. Rev. Lett. **13**, 508 (1964).
- [16] F. Englert and R. Brout, Phys. Rev. Lett. **13**, 321 (1964).
- [17] D. H. Lyth, Phys. Rev. Lett. **78**, 1861 (1997).
- [18] Herrera, R.: Phys. Rev. D **81**(2010)123511.
- [19] Del Campo, S. and Herrera, R.: Phys. Lett. B **660**(2008)282.
- [20] Setare, M.R. and Kamali, V.: JCAP **08**(2012).
- [21] Setare, M.R. and Kamali, V.: Phys. Rev. D **87**(2013)083524.
- [22] Bastero-Gil, M., Berera, A., Ramos, R.O., Rosa, J.G.: JCAP **1301**(2013)016.
- [23] M. Bastero-Gil, A. Berera, R.O. Ramos, J.G. Rosa: JCAP **1410**(2014)10053.
- [24] R. Herrera, M. Olivares and N. Videla: Eur. Phys. J. C **73**(2013)2295.
- [25] A. Jawad, S. Hussain, S. Rani and N. Videla, arXiv:1709.10430 [gr-qc].
- [26] Panotopoulos, G. and Videla, N.: Eur. Phys. J. C **75**(2015)525.
- [27] Jawad, A., Ilyas, A. and Rani, S.: Int. J. Mod. Phys. D **26**(2017)1750031; Astroparticle Phys. **81**(2016)61; Jawad, A., Rani, S. and Mohsaneen, S.: Eur. Phys. J. Plus **131**(2016)234; Astrophys. Space Sci. **361**(2016)158; Jawad, A., Butt, S. and Rani, S.: Astrophys. Space Sci. **361**(2016)258; Eur. Phys. J. C **76**(2016)274; Jawad, A., Rani, S. and Ilyas, A.: Int. J. Mod. Phys. D **26** (2017) 1750144.
- [28] Bamba, K. and Odintsov, S.D.: Eur. Phys. J. C **76**(2016)18; Bamba, K., Odintsov, S.D. and Tretyakov, P.V.: Eur. Phys. J. C **75**(2015)344; Sanchez, J. C. B., Bastero-Gil, M. Berera, A. and Dimopoulos, K.: Phys. Rev. D **77**(2008)123527; Herrera, R.: Phys. Rev. D **81**(2010)123511; Herrera, R. and San Martin, E.: Eur. Phys. J. C **71**(2011)1701; Herrera, R., Olivares, M. and Videla, N.: Eur. Phys. J. C **73**(2013)2295; Phys. Rev. D **88**(2013)063535.
- [29] Dimopoulos, K.: Phys. Lett. B **735**(2014)75.

- [30] Jawad, A., Ilyas, A. and Ahmad, S.: Int. J. Geom. Meth. Mod. Phys. **14**(2017)1750088; Jawad, A., Ilyas, A. and Rani, S.: Eur. Phys. J. C **77**(2017)131.
- [31] Kobayashi, T. and Seto, O.: Phys. Rev. D **89**(2014)103524.
- [32] Antonella cid, M., Del Campo, S., Herrera, R.: JCAP **0710**(2007)005.
- [33] Setare, M.R., Kamali, V.: JCAP **08**(2012).
- [34] Setare, M.R., Kamali, V.: Phys. Rev. D **87**(2013)083524.
- [35] Bastero-Gil, M., Berera, A., Ramos, R.O., Rosa, J.G.: JCAP **1301**(2013)016.
- [36] Y. Zhang, JCAP **0903**, 023 (2009).
- [37] M. Bastero-Gil, A. Berera, R. O. Ramos and J. G. Rosa, JCAP **1301**, 016 (2013).
- [38] A. Berera, M. Gleiser and R. O. Ramos, Phys. Rev. D **58** 123508 (1998).
- [39] Yokoyama, J. and Linde, A.: Phys. Rev D **60**, 083509, (1999).
- [40] Peebles, P. J. E. and Ratra, B. Rev. Mod. Phys. **75**, 559 (2003).
- [41] Ratra, B. and Peebles, P. J. E.: Phys.Rev. D **37**, 3406 (1988).
- [42] Caldwell, R.R., Dave, R. and Steinhardt, P. J.: Phys. Rev. Lett. **80**, 1582 (1998).
- [43] Sami, M. and Padmanabhan, T.: Phys. Rev. D **67**, 083509 (2003).
- [44] Armendariz-Picon, C., Mukhanov, C. and Steinhardt, P. J.: Phys. Rev. D **63**, 103510 (2001) .
- [45] Chiba, T.: Phys. Rev. D **66**, 063514 (2002) .
- [46] Scherrer, R. J.: Phys. Rev. Lett. **93**, 011301 (2004).
- [47] Sen, A.: J. High Energy Phys. **04**, 048 (2002) .
- [48] Sen, A.: J. High Energy Phys. **07**, 065 (2002) .

- [49] Gibbons, G.W.: Phys. Lett. B **537**, 1 (2002) .
- [50] Caldwell, R. R.: Phys. Lett. B **545**, 23 (2002) .
- [51] Elizade, E., Nojiri, S. and Odintsov, S.: Phys. Rev. D **70**, 043539 (2004).
- [52] Cline, J. M., Jeon, S. and Moore, G.D.: Phys. Rev. D **70**, 043543 (2004).
- [53] Kamenshchik, A., Moschella, U. and Pasquier, V.: Phys. Lett. B **511**, 265 (2001).
- [54] O. Bertolami and V. Duvvuri, Phys. Lett. B **640**, 121 (2006).
- [55] T. Barreiro and A. A. Sen, Phys. Rev. D **70**, 124013 (2004).
- [56] Li, M.: Phys. Lett. B **603**, 1 (2004).
- [57] Hinshaw, G., et al.: Astrophys. J. Suppl. **208**(2013)19.
- [58] Ade, P. A. R., et al.: A&A **594**(2016)A13.
- [59] Benaoum, H.B.: hep-th/0205140.
- [60] Gonzalez-Diaz, P.F.: Phys. Rev. D **68**(2003)021303.